DOI: 10.26599/FSHW.2025.9250827

Contents lists available at SciOpen

Food Science and Human Wellness

journal homepage: https://www.sciopen.com/journal/2097-0765

China Food Publishing Co.

Lactobacillus acidophilus Attenuates Ulcerative Colitis by Strengthening Intestinal Barrier Integrity and Modulating Microbiota-Immune Crosstalk

Liping Li[1,#], Jing Guo[1,#], Huan Li[1], Yangjun Shi[1],Shufen Guo[1],Wei Shi[1],Huan Yan[1], Xiaorong Shen[1], Jialu Liu[1], Yanyan Xu[1], Jin Huan Niu[1], Peng Ren[1], Xing Kang[1], Yuyu Qiao[1], Xinyue Chang[1], Yue Cai[1], Xiaohui Wang[2], Linzhi Guo[2], Ying Yang [3,*], Weiping Fan[1,*], Yongbo Kang [1, *]

[1] *Department of microbiology and immunology, School of Basic Medical Sciences, Shanxi Medical University, Taiyuan, Shanxi, China*

[2] *Laboratory of Morphology, Shanxi Medical University, Taiyuan, Shanxi, China*

[3] *Department of Endocrinology Affiliated Hospital of Yunnan University*

Kunming, Yunnan 650021, China

ABSTRACT: As a chronic idiopathic inflammatory disease that occurs primarily in the gastrointestinal tract, the cure rate for ulcerative colitis (UC) has been very low. UC has become a global public health issue with increasing incidence and recognition. Therefore, finding safe and effective drugs to treat UC is urgent. Meanwhile, different probiotics have demonstrated beneficial effects on this condition, thus increasing the interest in developing probiotic treatments. This study investigated the potential therapeutic effects of a novel *L. acidophilus* strain isolated from porcine guts on UC using a dextran sodium sulfate (DSS) induced mouse model. Treatment with *L. acidophilus* considerably alleviates colitis progression and restores the expression of intestinal barrier structures and functional proteins. Furthermore, the *L. acidophilus* increased the abundance of the symbiotic bacteria *norank_f__Muribaculaceae* and *norank_f__norank_o__Clostridia_UCG-014* while decreasing that of pathogenic *Escherichia-Shigella* to modulate directly microbial homeostasis. Mechanistically, the *L. acidophilus* largely regulates the expression of key regulatory proteins of TLR4/NF-κB, Nrf2/Keap1 and NLRP3/caspase-1 signaling pathways in colon tissue and regulates bile acid metabolism. Especially, *L. acidophilus* not only maintains the integrity of the intestinal barrier by upregulating the expression of tight junction proteins (TJPs), reduces metabolic endotoxemia, thereby inhibiting the activation of inflammatory signaling pathways and alleviating pathological symptoms such as damage to colonic epithelial cells and infiltration of inflammatory cells, but also modulates bile acid synthesis via the FXR/FGF15 signaling pathway, thus regulating the levels of cytokines and immune cell differentiation. In addition, microbiome phenotype prediction and bacterial functional potential prediction analysis demonstrated that the *L. acidophilus* supplementation regulated gut microbiota function involving inflammatory injury, metabolism, immune response, and pathopoiesia. Intriguingly, the *L. acidophilus* treatment restored the proportion of Th1/Th2 cells and Th17/Treg cells and the expression of specific inflammatory factors to maintain the immune balance, especially in intestinal epithelial cells. In conclusion, our results revealed that this novel *L. acidophilus* may have anti-inflammatory, antioxidant stress, anti-pyroptosis, regulation of bile acid metabolism, alleviation of endothelial dysfunction and intestinal dysbiosis effects, and it shows comparable efficacy to mesalazine in alleviating the

[#] These authors contributed equally to this work.
***Corresponding author**
Yongbo Kang, 657151276@qq.com
Ying Yang, yangying2072@126.com
Weiping Fan, weipingf@sxmu.edu.cn

Received 2 March 2025
Received in revised from 13 May 2025
Accepted 25 July 2025

pathological symptoms of UC mice. These findings provide theoretical guidance for the clinical treatment of *L. acidophilus* and pave the way for further exploration of its interaction with host immunity.

Keywords: *L. acidophilus*, Ulcerative colitis, Gut microbiota, Intestinal barrier function, Inflammation, Oxidative stress, Pyroptosis, Bile acid homeostasis

1. Introduction

Ulcerative colitis (UC) is an idiopathic intestinal inflammatory disease characterized by chronic inflammatory reactions and intestinal mucosal epithelial damage (1). Typical clinical symptoms are diarrhea, bloody stools, abdominal pain, and weight loss, and pathology describes numerous open ulcers and inflammatory infiltrations in the colon and rectum (2-5). Thus, the quality of life of patients with UC declines (6), and without intervention, patients with long-term UC are more likely to develop colorectal cancer (CRC) (7), which has become a top medical concern for medical personnel (8). 5-aminosalicylate (5-ASA), glucocorticosteroids, azathioprine, and cyclosporine are used to treat UC in clinical. However, they are not the best treatment option due to their low cure and high recurrence rates (9). Furthermore, with the rapid development of industrialization and modernization, the incidence of UC is increasing in Asia (10). Nevertheless, the pathogenesis of UC is multifactorial, which is essentially the result of genetic predisposition (2), immune dysregulation (11, 12), intestinal barrier defects, and microbial disorder (13, 14).

The emerging evidence indicates that intestinal mucosal barrier damage, intestinal microbiome disturbance, and immune homeostasis imbalance are closely related to the occurrence of UC (15, 16). Damage to the intestinal mucosal barrier is considered to be a pivotal factor in high susceptibility to UC, manifested by the breakdown of tight junction structure and goblet cells leading to leakage of inflammatory substances, which leads to the activation of TLR4/NF-kB pathway, accelerates the expression of a large number of inflammatory factors, disrupts immune system homeostasis, and ultimately aggravates intestinal mucosal inflammation (17, 18). UC is related to the inflammatory response driven by the overactivation of immune cells and the secretion of inflammatory factors (19). In addition, pro-inflammatory cytokines can induce redox-sensitive transcription factors to increase inflammation through the production of oxidation products and eventually destroy the intestinal barrier, thus changing the redox balance of intestinal mucosa (20). Simultaneously, more researchers showed that Nrf2/Keap1 pathway plays a key role in inducing antioxidant stress and regulating inflammatory response. It has been confirmed that NLRP3 inflammasome activation induced pyroptosis can promote the progression of UC (21, 22). Bile acids (BAs) have been reported to regulate various physiological activities and immune responses. Accumulating evidence has suggested that abnormal BAs metabolism is associated with the development of UC and that FXR plays a vital role in regulating the degree of inflammatory response, barrier function and prevention of bacterial translocation in the gut (23). Given that, there is an urgent need to explore more novel, efficient and safe therapeutic strategies to prevent and treat UC.

Probiotics have been defined and are now ubiquitously referred to as “live microorganisms,” which must be administered in adequate amounts to provide the health benefits for the host. Since probiotics have been

found to change the composition of the gut microbiota and improve host health, they are considered to be an important strategy for maintaining intestinal homeostasis (24-26). Besides, growing evidence has indicated that probiotics may be the most effective way to treat UC by regulating the gut microbiota balance without side effects (27-30). Among the probiotics, *Lactobacillus* is relevant to treating inflammatory diseases to the greatest extent, and show considerable anti-inflammatory effects in rodents and humans (31, 32). Accumulating studies have demonstrated that *L. acidophilus* can increase body weight, food and water intake, improving intestinal damage and microbial imbalance, reduce aberrant inflammatory responses and thereby effectively alleviate the pathological symptoms of UC(33). Its beneficial effects may involve multiple mechanisms, including increasing the beneficial bacteria that produce short chain fatty acids (SCFA), maintaining intestinal intraepithelial immune homeostasis and protecting the host from metabolic endotoxemia, most likely by regulating the gut microbiota(25). In this context, the recognition that *Lactobacillus* can be used as an alternative therapy to improve UC and related inflammatory diseases has been recognized by more and more researchers. However, the underlying molecular mechanism of the action of probiotics remains to be elucidated.

At present, although some studies have demonstrated that *L. acidophilus* can alleviate UC, their efficacy has not been compared with that of clinical drugs. Meanwhile, these strains are mainly isolated from humans and food. In addition, the available strains of *L. acidophilus* for UC treatment remain limited, highlighting the pressing need to identify more effective and stable strains for UC management. Recently, a study has found that native domestic pigs in China exhibit a stable and resilient intestinal microbiota and demonstrate strong resistance to UC (34). Hence, we attempted to isolate the novel *L. acidophilus* strains from pig intestines to investigate their potential therapeutic effects on UC.

Consequently, the primary objective of this study is to determine the efficacy of a novel *L. acidophilus* species isolated from the pig intestine in the mouse model of dextran sulfate sodium (DSS)-induced UC to establish the anti-inflammatory effect and its effect on intestinal barrier and flora stability. Additionally, the influence of physiological and pathological changes in colitis, intestinal barrier function, intestinal microflora and their metabolites, immune responses, pyroptosis and oxidative state, and the relevant molecular signaling pathways are explored. Ultimately, these experimental results have confirmed the great potential of probiotic *L. acidophilus* in the clinical application, and provide favorable scientific evidence for the clinical application of *L. acidophilus* in UC.

2. Materials and methods

2.1. Preparation and administration of probiotics

The probiotic *L. acidophilus* (Genbank accession numbers: OL457299) was isolated from porcine guts and stored in the Department of microbiology and immunology, School of Basic Medical Sciences, Shanxi Medical University (China, Shanxi). Then, it was grown in DeMan, Rogosa and Sharpe (MRS) media for 48 h at 37 ◦C under anaerobic conditions using the Anaerogen system (Oxoid, Basingstoke, UK). After that, cultured cells (Bacteria) were harvested by centrifugation (2000 g, 4 ◦C, 10 min), washed three times with

sterile phosphate buffered saline (PBS), and then resuspended in sterile PBS. For probiotic treatment, it was suspended using a sterile PBS solution and was diluted to obtain a concentration of 1×10^9 CFUs in 1 ml.

2.2. Animal experiments and design

All animal experiments were approved by the Ethics Committee of Shanxi Medical University (Shanxi, China). Six-week-old C57BL/6 male mice obtained from Beijing HuaFuKang Laboratory Animal Co., Ltd. (Beijing, China) were kept in an environment without pathogens under the condition of 21–25 ℃ and 55 ± 10% humidity on a 12-h light/dark cycle. Mice were provided with distilled water and food ad libitum in the meantime. After one week of acclimation, the mice were randomly divided into four groups: control group (n = 7), dextran sulfate sodium (DSS) group (n = 7), mesalazine (DSS-AS) group (n = 7) and probiotics (DSS-LA) group (n = 7). The experimental flow is graphically illustrated in (Figure 1a). From day 1 to day 8, mice in the 3 treatment groups were provided with 3.0% (wt/vol) DSS (MP Biomedicals, Santa Ana, CA, USA, molecular weight of 36,000–50,000) dissolved in distilled water to establish a UC model. From day 8 to day 16, In the Ctrl and DSS group, mice were given 200 μl PBS by gavage, while mice in the DSS-AS group and DSS-LA group were orally administrated with mesalazine (Adisha, H20143164, 1mg/kg/per/day) and probiotics, respectively. And throughout the treatment period, the body weight, food intake, water intake, and DAI (Table 1) were recorded daily as indicators of the success of UC model construction and probiotics or ASA treatment. Apart from that, the intestinal permeability test in vivo was conducted on 17 days. Then, all the mice were sacrificed under anesthesia, blood samples were centrifuged at 3,000 r/min at 4℃ for 15 min to obtain the serum, and serum samples were stored at −80 ℃. Immune organs were collected and weighed. Liver, ileum, and colon tissues were either fixed in 4% paraformaldehyde for immunohistochemical and histological examination or frozen at–80℃.

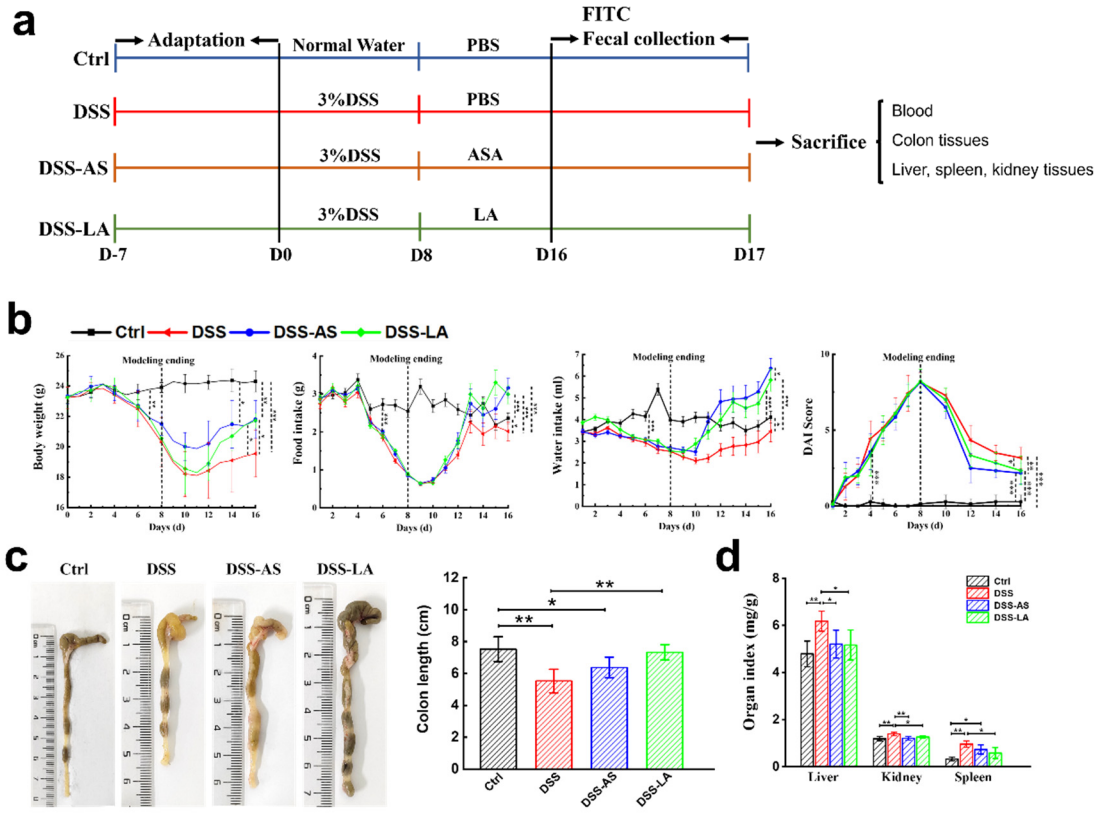

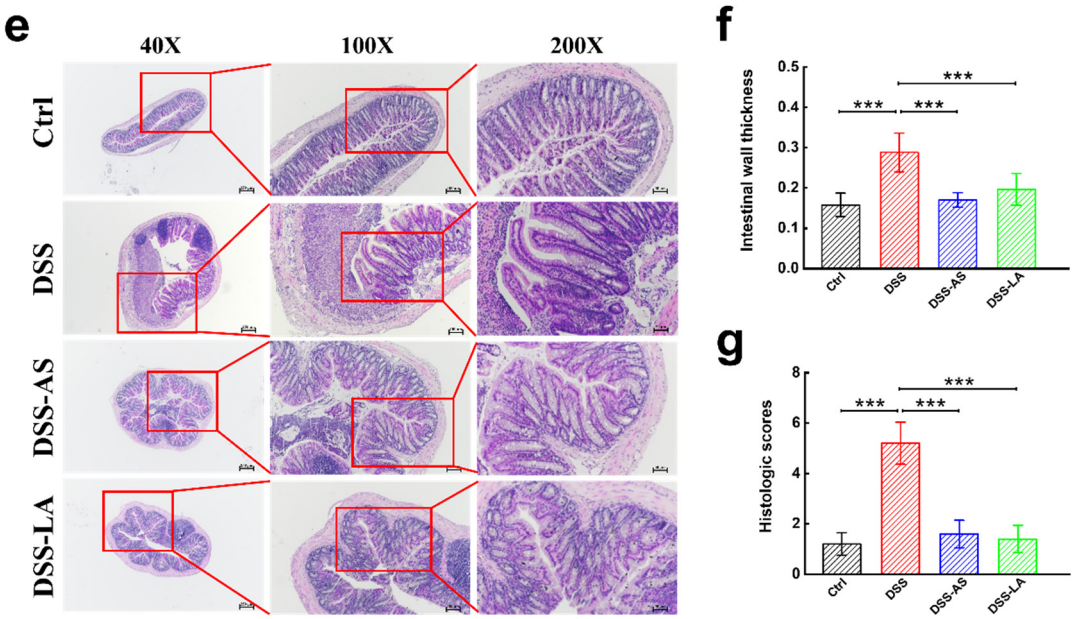

Figure 1. Effect of *L. acidophilus* on clinical symptoms and pathological injury in mice with DSS induced colitis. (a) Experimental design grouping and timeline. Effects of *L. acidophilus* treatment on (b) physiological changes : body weight, food intake, water intake and disease activity index, ("Modeling ending" refers to the end date of modeling UC with DSS on days 1 to 8; no DSS water was administered to mice beginning with day 9); (c) representative image and section of colon tissue in each group and Colon length (cm); (d) The immune organ index (mg/g) of mouse liver, kidney and spleen. The immune organ index is calculated as immune organ index = immune organ weight (mg)/body weight; (e) Representative histological observation of hematoxylin & eosin-stained mouse colon at magnifications of 40, 100, and 200; (f) Intestinal wall thickness (mm); (g) Histopathological scoring of colon tissue. Data are expressed as means ± SEM (n = 7). ns > 0.05; * $P < 0.05$; * * $P < 0.01$ and * ** $P < 0.001$. Color code for animal groups: Ctrl, black DSS, red; DSS-AS: blue; DSS-SY, green.

Table 1. Disease activity index (DAI) scoring system of dextran sodium sulfate-induced colitis

Score	Weight	Stool consistency	Bloody stool
0	Decrease 0%	Normal	Negative for FOBT
1	Decrease 1~5%	Loose state, which is pasty and semi-formed stool that does not adhere to anus	Positive for FOBT
2	Decrease 6~10%	Obvious loose state, which is a pasty and basically unformed stool that does not adhere to the anus	Strongly positive for FOBT
3	Decrease 11~15%	Dilute stool is a watery stool that can adhere to the anus	Visible bloody stool
4	Decrease ≥16%	The degree of loose stool is more obvious, and the thin water sample is more clear and long	Obvious visible bloody stool

2.3. FITC-dextran permeability assay

The intestinal permeability of mice was evaluated by oral administration of fluorescein isothiocyanate-labeled dextran (FITC-dextran, 4 kDa, New Research Biosciences Co., Ltd., Xian, China) described previously (35). At the beginning of the experiment, mice were fasted for 4 h and then intestinal permeability was tracked by intragastric administration of FITC-dextran at 600mg/kg body weight. Serum was harvested after 4h, centrifuged (4℃, 3000 r/min, 10 min) to obtain the supernatant, followed by being diluted by adding 5 volumes of PBS and detected by microplate spectrofluorometer (excitation, 490 nm; emission, 520 nm; SpectraMax iD3, USA). Finally, a standard curve for evaluating the concentrations of FITC-dextran in each sample was made by diluting the FITC-dextran standard with PBS (1:9 [vol/vol]).

2.4. Histological analysis

2.4.1. Histological analysis (HE)

Tissues of the distal colon and liver of mice were fixed in 4% paraformaldehyde overnight, dehydrated in gradient ethanol, embedded in paraffin, sliced into 3 μm sections, stained with hematoxylin and eosin. Subsequently, Images were observed for histopathological changes under a microscope (AxioObser Z1, Germany) to assess histological damage scores by referring to the method (36) (Table 2). The Image-J analysis software was used to measure the thickness of the colon mucosal layer in a unified millimeter standard unit at 6 positions of each layer from the right first, and then the average value was calculated.

Table 2. Histopathology scoring system of dextran sodium sulfate-induced colitis

Project	Degree	Score
Cryp damage	None	0
	1/3 cryptofbasementwasdestroyed	1
	2/3 cryptofbasementwasdestroyed	2
	Onlyintactsurfacccpithclium	3
	Allcryptsandepitheliumwere destroyed	4
Goblet cell loss (%)	0	0
	1~25	1
	26~50	2
	51~75	3
	76~100	4
Inflammation	None	0
	Mildorfew	1
	Moderate	2
	Severemassive	3
	Extremclyscvcrcandmassive	4
Range of inflammation (%)	0	0
	1~25	1
	26~50	2
	51~75	3
	76~100	4
Depth of inflammation	None	0
	Submucosallayer	1
	Muscularlayer	2
	Serouslayer	3
	Transmural	4

2.4.2. Alcian blue and PAS staining

The sections (3 μm) were deparaffinized in xylene, rehydrated in decreasing concentrations of ethanol, and then stained with the Alcian blue kit (Solarbio Science & Technology Ltd. Beijing, China) and PAS kit (Leagene Biotechnology Co., Ltd. Beijing, China). Then, the positive areas observed under the microscope (AxioObser Z1, Germany) by Alcian blue and PAS staining are blue and red, respectively, which were calculated by Image-J software and divided by the total area of the section. Finally, the result was given as a% area of the section stained positively for Alcian blue and PAS.

2.4.3. Oil-Red-O staining

To evaluate the lipids within liver tissues, frozen sections were stained with the Oil Red O Saturated Solution (Solarbio, China). Frozen tissue was embedded in optimal cutting temperature (OCT) and snap-frozen. The obtained frozen sections (7-μm-thick) were fixed in Formaldehyde-Calcium Fixative for 10 min and then rinsed with 60% isopropanol, stained with Oil Red O Working Solution for 10 min. Finally, the sections were differentiated by 60% isopropanol and re-dyeing with hematoxylin for 3 min.

2.5. Immunohistochemical and Immunofluorescence Staining

The colon and liver tissue were fixed for 24 h, dehydrated in gradient ethanol, embedded in paraffin, and sliced into 3 μm sections that were then deparaffinized, rehydrated, and washed in PBS. The sections were immersed in the citrate buffer (pH 6.0) for 10 min using microwaves to retrieve antigen. The sections were then blocked with 5% bovine serum albumin for 30 minutes at room temperature, followed by being stained overnight with the different primary antibodies. For immunohistochemical staining, sections were incubated at 4℃ overnight with antibodies against Nrf2 (CST, USA), Keap-1 (CST, USA), NLRP3 (Abmart, China), pro-caspase-1 (Abcam, UK), cleaved-caspase-1 (CST, USA), caspase-1 (Abcam, UK), ASC (Elabscience, China), GSDMD-N (Bioss, China), FXR (Proteintech, China), CYP7A1(Bioss, China) and FGF15 (Abmart, China), also incubated with the corresponding secondary antibodies for 30 minutes at room temperature the next day and stained with 3, 3′-diaminobenzidine. Furthermore, images were obtained under a microscope (AxioObser Z1, Germany) and positive results were quantified using ImageJ software. For immunofluorescence on tissues, primary antibodies ZO-1(Abcam, UK) and occludin (Abcam, UK) were used for incubation overnight at 4℃, and followed by fluorescent secondary antibodies coupled with Alexa Fluor 555 (BBI, China) for incubation at room temperature and darkness for 30 min. Nuclear were stained with DAPI (Bioss, China). Eventually, the position staining of the sections was observed as red signals under a fluorescence microscope (Nikon, Japan), quantified by ImageJ software.

2.6. Enzyme-linked immunosorbent assay (ELISA)

Inflammatory markers in mouse serum were determined using IL-4, IL-6, IL-10, IL-18, IFN-γ, IL-17, IL-1β, IL-22, IL-23, TNF-α and MPO kits ((X-Y Biotechnology, Shanghai, China), and all steps were performed strictly according to the manufacturer instructions. The absorbance was measured at 450 nm using an enzyme marker (Spectra Max i3x, Molecular Device, USA). Other than that, SOD, MDA, GSH-Px and CAT activities in the colon tissue were detected using ELISA methods to evaluate the degree of oxidative stress, according to the instruction of the commercial kits, as previously described (37).

2.7. Quantitative real-time PCR

Total RNA from colonic and liver samples was extracted and purified using Trizol (Seven, China), following the manufacturer's recommendations and reverse-transcribed into cDNA using the MonScript RTIII Mix (Monad, China). In addition, real time quantitative PCR amplification and detection were performed by using the MonAmp SYBR Green qPCR Mix (Monad, China), and then the QuantStudio 3 systems (Applied Biosystems, USA) were used for RT-PCR analyses. The primers for RT-PCR are listed in

Table 3. Moreover, Relative gene expression levels were presented as the mean ± SEM normalized to β-actin expression using the ΔΔCt method.

Table 3. Primer Sequence in RT-PCR

Gene Name	Forward Sequence 5′~3′	Reverse Sequence 5′~3′
β-actin	CACTGTCGAGTCGCGTCC	TCATCCATGGCGAACTGGTG
CYP7A1	CTACTTCTGCGAAGGCATTTGG	AGGCATACATCCCTTCCGTG
FXR	TGGGTACCAGGGAGAGACTG	GTGAGCGCGTTGTAGTGGTA
Occludin	GCGGAAGAGGTTGACAGTCC	ACTCCCCACCTGTCGTGTAG
ZO-1	CAGCCGCATCTTCTTGTG	AGGAGCGAGACCCCACTAA
ZO-2	AACGGATGCTGGAAGTTAAT	TCTGCTTGCTGTCTCTCAACA
Claudin-1	CTG TGG ATG TCC TGC GTT TC	TCA TGC ACT TCA TGC CAA TG

2.8. Western blot analysis

Western blot was performed according to previously described method (38). Protein samples from colon and liver were prepared, subjected to 10% SDS-PAGE, and then transferred to the PVDF membrane, which was probed with the corresponding primary antibodies against TLR4 (Bioss, China), NF-κB p65 (Bioss, China), phosphor-NF-κB p65 (Bioss, China), IκB (Bioss, China), phosphor-IκB (Bioss, China), FXR (Proteintech, China), FGF15 (Abmart, China) and β-actin (BBI, China) at 4 ℃ overnight, and then incubated with 1 : 10000 for goat anti-rabbit IgG-HRP (BBI, China) at room temperature for 1 h. Moreover, the target bands were detected by enhanced chemiluminescence (ECL; Seven, China). The stained membranes were quantified by employing the Tanon imaging system, and Image-J software was used to analyze the densitometric of the target bands.

2.9. Flow cytometry analysis

Detailed operational steps for this procedure are outlined in our previous research (39). Briefly, after animals were humanely sacrificed, the spleen was placed on a 200-mesh sieve moistened with PBS, and a 1mL syringe was used to draw the pre-cooled PBS solution into the spleen and swell the membrane for collection of the spleen cell suspension. After adding erythrocyte lysate, the suspension was centrifuged and the supernatant was discarded. The cells were washed with PBS, and 1mL of culture solution containing 10% fetal bovine serum (FBS) was added to the precipitated cells. The cells were counted, and the cell concentration was adjusted to 1.0 × 107 per mL. To detect Th1, Th2, Th17 and Treg cells, 1 mL of single cells were seeded per well in 6-well plates; they were then incubated with ionomycin (500 ng/mL), PMA (5 ng/mL), and Brefeldin A (1 μg/mL) for 5 h and harvested. The harvested cells were stained with APC-conjugated anti-mouse CD4 at room temperature in the dark for 30 min and incubated with CytoFix/Cyto Perm buffer (BD Biosciences, USA) at room temperature for 15 min. Finally, they were stained with anti-IFN-γ-FITC mAb, anti-IL-4-PE mAb, FITC-IL-17A mAb and PE-Foxp3 mAb (BD Biosciences, USA), incubated at room temperature in the dark for 30 min, and analyzed by FACS. Data were analyzed using FlowJo software (BD Biosciences, USA). Lamina propria cells (LPCs) were prepared by consulting the method of Xie (40). In brief, the intestinal cavity was cut into 0.5 cm fragments after rinsing the contents with PBS. Then, the fragments were immersed in PBS digestive solution containing 5 mmol/L EDTA and 4%

serum and digested at 37 ℃ on a shaker with 250 r/min for 20 min to release the epithelial cells. Afterwards, LPCs were isolated from the intestine pieces through the treatment of RPMI1640 medium digestion solution containing 4% FBS, collagenase-D (0.5 mg/mL), DNase I (0.5 mg/mL) and Dispase (1 mg/mL) for 20 min at 37 ℃. The concentration of LPCs was adjusted to 1×10^6 cells per mL with PBS-5% FBS and incubated with anti-CD4-APC, anti-IFN-γ-FITC, anti-IL-4-PE or anti-IL-17A-PE to analyze Th1, Th2 and Th17 cells, and with anti-CD4-APC and anti-Foxp3-PE to analyze Treg cells using a 14-color BD LSR Fortessa flow cytometer (BD Biosciences, San Jose, CA, USA).

2.10. Intestinal microflora analysis

The gut microbial diversity of stool specimens was analyzed according to our previous study.(25) The DNA of feces (n = 7 per group) was derived according to the manufacturer's instructions (E.Z.N.A. ® Soil DNA Kit, Omega, USA). The 16S rRNA gene sequencing of DNA samples was undertaken by Majorbio Bio-Pharm Technology Co., Ltd. (Shanghai, China). In addition, the primers of the variable regions V3 − V4 are as follows: 338F, 5′-ACTCCTACGGGAGGCAGCAG-3′ and 806R, 5′-GGACTACHVGGGTWTCTAAT-3′ (ABI GeneAmp® 9700 PCR thermocycler, USA). After that, bioinformatic analysis was analyzed on an online platform, Majorbio Cloud Platform (https://www.majorbio.com). The specific analysis method is as follows: Alpha diversity indices and bacterial abundance data of different groups were compared by performing the Kruskal–Wallis test followed by Mann–Whitney U test. Then, resulting *p*-values were corrected with the Bonferroni method. In addition, a Venn diagram was depicted to show core intestinal flora species, and Beta diversity analysis was conducted to investigate the structural variation of microbial communities across samples using UniFrac distance metrics and visualized via principal coordinate analysis (PCoA). Besides, differences in the UniFrac distances among groups were determined by analyzing similarities (ANOSIM). To compare the relative levels of abundant taxa at the phylum, family, and genus levels among the groups, the one-way analysis of variance (ANOVA) and post-hoc least significance tests were carried out by IBM SPSS Statistics software 19.0. Other than that, LEfSe (linear discriminant analysis (LDA) effect size) was performed to identify biomarkers for both abundant taxa and functional pathways by calculating the LDA score (more than 4) across groups, while the heatmap was plotted using R package 3.3.1. A bacterial Co-occurrence network analysis was constructed by Networkx (version1.11). Meanwhile, Circos map visualizes the species-sample relationship by Circos-0.67-7 (http://circos.ca/). Furthermore, Phylogenetic Investigation of Communities by Reconstruction of Unobserved States (PICRUSt) based on OTUs was employed to predict the abundances of functional categories using Kyoto Encyclopedia of Genes and Genomes (KEGG) orthologs (KO), and at the same time, BugBase was adopted to forecast bacterial composition based on the sequencing results. Furthermore, Pearson's correlation analyses were made to assess correlations between taxa and the factors, whilst the data are expressed as the mean ± standard error of the mean (SEM), and $P < 0.05$ was the threshold of significance.

2.11. Data analysis

Statistical analysis was performed using SPSS software (IBM SPSS version 19.0), and figures were generated utilizing Origin software (Origin 2019b). These results were analyzed using one-way analysis of variance (ANOVA) followed by the Least Significant Difference (LSD) post hoc test and Dunnett's T3 post hoc test. Error bars correspond to standard error of mean (SEM). P value < 0.05 was considered significant.

3. Results

3.1 L. acidophilus ameliorated DSS-induced colitis symptoms in mice

DSS-induced impaired intestinal function in UC mice is characterized by malabsorption, decreased appetite, weight loss, diarrhea, and bloody stools (5, 41, 42). Accordingly, from days 1 to 8, compared with the control group, the lower the body weight, the lower the amount of water and food intake and the higher the disease activity index (DAI) score (the scoring criteria are shown in Table 1) were showed in the DSS group, DSS-AS group and DSS-LA group (Figure 1b), and the blood red feces of the mice were observed in this three group (Supplementary Figure 1a). In brief, these indicators serve as the preliminary judgment criteria for the success of UC model construction. Then, on days 9 to 16, the body weight, the food intake and the water intake of the DSS-AS group and DSS-LA group gradually increased, but the DSS group did not increase as significantly as in the two groups. Furthermore, after stopping drinking DSS on day 8, the remission effect on UC in the DSS-AS group and DSS-LA group was much greater than the self-healing range in the DSS group, suggesting that this probiotic *L. acidophilus* and ASA can greatly promote the recovery of UC (Figure 1b).

In colitis, the immune organ index will be increased to varying degrees, and the length of the colon will be severely shortened (43). Our results also showed that the immune organ index was significantly increased, the colon length was significantly shortened, and the colonic cavity widened, bleeding points increased, and mucosal shedding in the DSS group. However, intake of *L. acidophilus* and ASA inhibited the elevation of immune organ index, prevented the bleeding and shortening of colon, and obviously alleviated the DSS-induced colitis symptoms (Figure 1c and d). Moreover, histopathological analysis revealed that colon tissue in DSS group underwent severe injury, including significant inflammatory cell infiltration, structural damage to the intestinal mucosa with focal villus edema, loss of goblet cells and crypts, and significantly increased intestinal wall thickness and morphological scores, which were improved to different degrees by the administration of *L. acidophilus* and ASA (Figure 1e-g).

In addition, previous studies have shown that DSS induced UC mice will show symptoms such as lethargy, abdominal pain, arched back and panic as the course of the disease worsens, and the spleen will also be congested and edema, infection and blackening (44, 45). Consistent with the results mentioned above, compared with the normal group, on the eighth day, we observed that the DSS, DSS-AS, and DSS-LA group of mice developed yellow and smelly urine, blood in the stool and difficulty in defecation, dry hair curling, slow reaction, easy to panic, arched back and reduced body size, After the treatment of *L. acidophilus* and ASA, on the 16th day, the mental state of the mice was improved, lively and active, no hematochezia and arched back, and the hair was soft and shiny, while the mental state of the mice in the DSS group was still poor (Supplementary Figure 1b). Simultaneously, we also found that the spleens of mice in the DSS group were

obviously larger than those in the control group, and gradually returned to normal after the intervention of the *L. acidophilus* and ASA (Supplementary Figure 1c). Overall, these results emphasize the palliative effect of the *L. acidophilus* on UC is comparable to that of ASA and has excellent application value.

3.2 L. acidophilus protected the integrity of intestinal barrier function in colitis mice

It was well known that the expansion of intestinal inflammation and subsequent destruction of the functional structure of the epithelial barrier is a primary pathological feature of UC. As expected, the FITC-dextran permeability experiment showed that DSS drinking dramatically increased intestinal permeability (plasma FITC-dextran), which were completely restored by the *L. acidophilus* treatment (Figure 2a). In addition, tight junction proteins (TJPs), including ZO-1, ZO-2, and Occludin, play a crucial role in maintaining the integrity of the intestinal barrier. They selectively regulate the permeation of nutrients and water while establishing an endothelial barrier to effectively block pathogens from paracellular entry (25, 46). In this experiment, we observed a significant down-regulation of colonic TJPs and gene expressions of ZO-1 and Occludin in the DSS group of mice. Additionally, there was a notable decrease in gene levels of ZO-2, which may play a crucial role in the progression of UC disease. However, treatment with *L. acidophilus* demonstrated a significant ability to prevent the reduced expression of these tight-linking proteins, restore intestinal barrier integrity, and attenuate inflammatory response (Figure 2b, c, d, f, g).

More importantly, the mucus layer that envelops the surface of intestinal epithelial cells is composed of a complex macromolecular glycoprotein secreted by specialized columnar goblet cells interspersed within the lining of the intestinal epithelium. This mucus barrier plays a crucial role in safeguarding and preserving the integrity of the intestinal mucosa (47, 48). Consequently, the quantity of goblet cells directly impacts the functionality of the intestinal barrier. Compared to the normal group, the DSS group exhibited a significant reduction in goblet cells and their associated mucin secretion as evidenced by Alcian blue staining and PAS staining, whereas an increase was observed in the DSS-LA group and DSS-AS group. This phenomenon is consistent with the analytical results of HE staining mentioned above (Figure 2e).

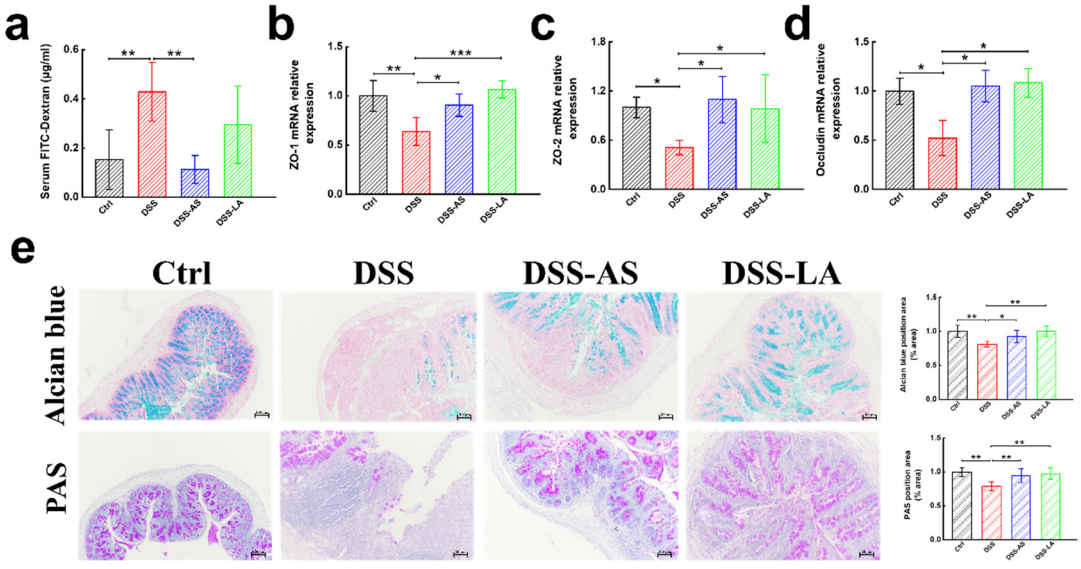

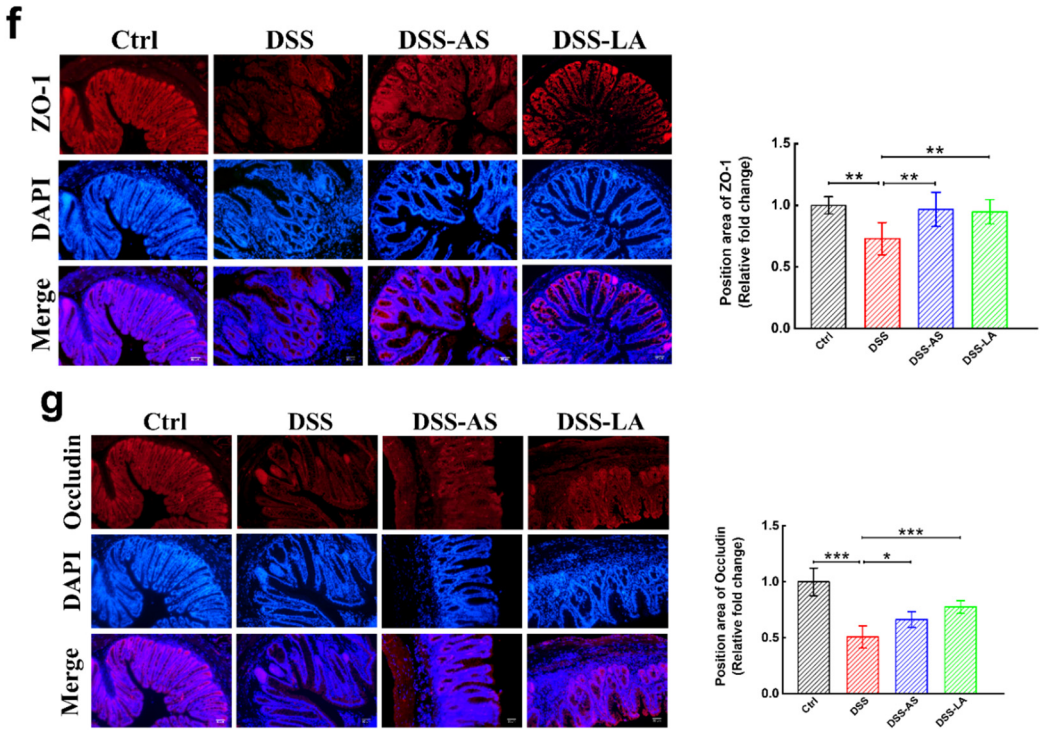

Figure 2. Effects of *L. acidophilus* on intestinal barrier structure and function in colitis mice. (a) Intestinal permeability assay: Plasma DX-4000-FITC (μg/ml); (b) Relative expression of gene ZO-1; (c) Relative expression of gene ZO-2; (d) Relative expression of gene Occludin; (e) Representative images of colon tissue Alcian blue staining and PAS staining and quantification of the area of position staining, Scale bar = 100 μm; (f) Representative images of colon tissue ZO-1 protein immunofluorescent staining and position area, Scale bar = 50 μm; (g) Representative images of colon tissue Occludin protein immunofluorescent staining and position area, Scale bar = 50 μm. Data are expressed as means ± SEM (n = 7). ns > 0.05; * $P < 0.05$; * * $P < 0.01$ and * ** $P < 0.001$.

3.3 L. acidophilus modulated the intestinal microbiota in colitis mice

The gut microbiota of individuals with UC and mice induced with DSS exhibit a reduction in α diversity, alterations in β diversity, an increased ratio of Firmicutes to Bacteroidetes, elevated levels of endotoxin-producing bacteria, and a decrease in immuno-homeostatic bacterial species (27, 49-52). Considering this, the impact of *L. acidophilus* supplementation on the composition of gut microbiota was assessed through a MiSeq sequencing-based analysis targeting the V3-V5 region of bacterial 16S rRNA in fecal samples.

3.3.1. Effects of L. acidophilus supplement on gut microbial diversity and richness

In assessing gut microbial α diversity metrics, richness and evenness were considered by incorporating the Chao, ACE, Simpson, and Shannon indexes. It is well known that the Chao index and ACE index are related to richness, while the Simpson Index and Shannon index are related to evenness. Consumption of DSS significantly reduced gut microbial α diversity, whereas *L. acidophilus* treatment fully restored this influence (Figure 3a, Supplementary Figure 2a and b). In order to gain a deeper comprehension of the shared richness among each group, we present a Venn diagram featuring overlapping circles to visually depict the extent of overlap between groups. Subsequently, it is demonstrated that out of the total richness of 2075 OTUs, only 170 were found to be shared across all groups, while there existed a greater number of OTUs among three groups, between two groups, or within each group. Furthermore, supplementation with *L. acidophilus*

significantly augmented the abundance of OTUs in DSS mice (Figure 3b). Besides, β diversity quantifies the dissimilarity between microbial communities through principal component analysis (PCA) and principal coordinate analysis (PCOA), wherein the proximity of distinct color points reflects similarity in their respective bacterial community structures. Notably, dots tend to form clusters within their own groups. The result revealed significant differences in the overall composition of intestinal flora among different groups (Figure 3c, Supplementary Figure 2c). Collectively, these results boil down to the fact that probiotic *L. acidophilus* interventions can significantly increase the richness and diversity of gut microbiota.

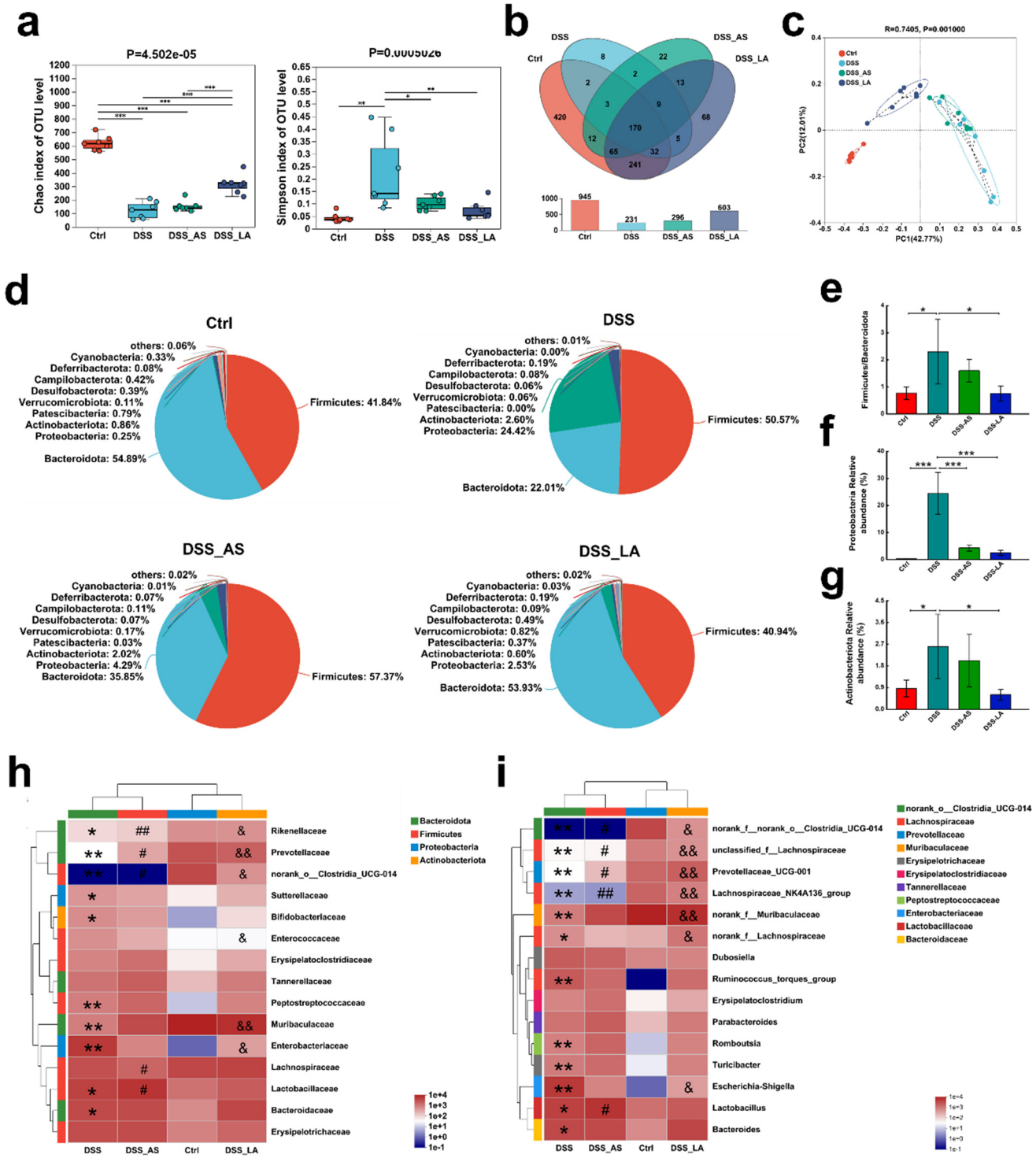

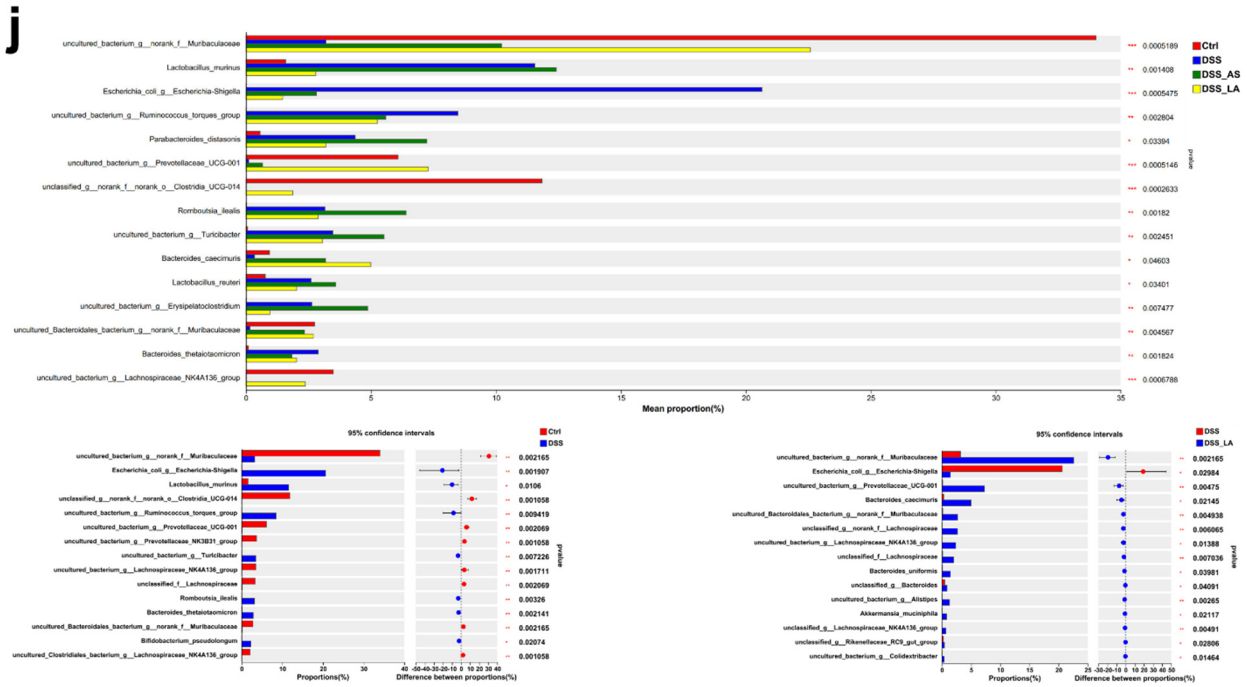

Figure 3. Effects of *L. acidophilus* on intestinal microbial composition in colitis mice. Effects of *L. acidophilus* treatment on α-diversity was determined using (a) Chao index and Simpson index; (b) Venn diagram illustrated overlap of OTUs in intestinal microbiota among the samples; (c) β-diversity was determined using Euclidean distance based Principal Component Analysis (PCA); (d) The average relative abundance of the major microbial phyla; (e) The Firmicutes to Bacteroidetes ratio; (f) Relative abundance of Proteobacteria; (g) Relative abundance of Actinobacteriota; (h) Relative abundance of the top 15 different family; (i) Relative abundance of the top 15 different genera; (j) Relative abundance of the top 15 different species. Data are expressed as means ± SEM (n = 7). ns > 0.05; * $P < 0.05$; * * $P < 0.01$ and * ** $P < 0.001$ versus Ctrl; & $P < 0.05$, && $P < 0.01$ and &&& $P < 0.001$ versus DSS; # $P < 0.05$, ## $P < 0.01$ and ### $P < 0.001$ versus DSS-SY.

3.3.2. Effects of L. acidophilus supplement on the gut microbiota composition

Numerous studies have shown that the occurrence and development of UC are closely related to the decrease of bacterial flora abundance and disproportionate number of probiotics and harmful bacteria (53, 54). Under the circumstances, by taxonomic classification analysis of the composition of gut microbes at the phyla, family, genus, and species level, we found that Firmicutes, Bacteroidetes, Proteobacteria, and Actinobacteria primarily dominated the gut microbiota in mice (Figure 3d, Supplementary Figure 2d). Accordingly, the ratio of Firmicutes/Bacteroidetes and the relative abundance of Proteobacteria and Actinobacteriota in the model group significantly increased. It is worth noting that the addition of *L. acidophilus* significantly reduced these effects, and the treatment effect of Lactobacillus acidophilus on Firmicutes/Bacteroidetes and Actinobacteria was significantly stronger than that of the positive drug ASA, demonstrating the strong regulatory potential of probiotic (Figure 3e-g). In the top 15 families, ten genera were remarkably impacted by the DSS. Compared with the Ctrl group, the DSS group had increased relative abundances of Sutterellaceae, Bifidobacteriaceae, Peptostreptococcaceae, Enterobacteriaceae, Lactobacillaceae and Bacteroidaceae significantly increased, whereas Rikenellaceae, Prevotellaceae, norank_o__Clostridia_UCG-014 and Muribaculaceae were decreased drastically. Strikingly, *L. acidophilus* supplement considerably restored Rikenellaceae, Prevotellaceae, norank_o__Clostridia_UCG-014, and Muribaculaceae levels, while reducing the relative abundance of Enterococcaceae and Enterobacteriaceae. It

is worth noting that compared with the DSS-LA group, the relative abundance of Lactobacillaceae in the DSS-AS group was observably increased in the DSS-AS group, while the relative abundance of Rikenellaceae, Prevotellaceae, norank_o__Clostridia_UCG-014 and Lachnospiraceae was decreased visually. (Figure 3h).

Subsequently, up to 12 of the first 15 genera were significantly affected by DSS. Compared with the control group, the DSS group had increased relative abundances of *norank_f__Lachnospiraceae*, *Ruminococcus_torques_group*, *Romboutsia*, *Turicibacter*, *Escherichia-Shigella*, *Lactobacillus* and *Bacteroides* significantly increased, whereas *norank_f__norank_o__Clostridia*_UCG-014, unclassified*_f__Lachnospiraceae*, *Prevotellaceae*_UCG-001, *Lachnospiraceae*_NK4A136_group and *norank_f__Muribaculaceae* were decreased remarkably. Surprisingly, *L. acidophilus* supplement significantly enhanced *norank_f__norank_o__Clostridia*_UCG-014*,* unclassified*_f__Lachnospiraceae, Prevotellaceae*_UCG-001*,* *Lachnospiraceae*_NK4A136*_group*, *norank_f__Muribaculaceae* and *norank_f__Lachnospiraceae* levels, while decreasing the relative abundance of *Escherichia-Shigella*. Besides, compared with the DSS-LA group, the relative abundances of *Lactobacillus* in the DSS-AS group were evidently increased, while the relative abundance of *norank_f__norank_o__Clostridia*_UCG-014*,* unclassified*_f__Lachnospiraceae, Prevotellaceae*_UCG-001*,* and *Lachnospiraceae*_NK4A136*_group* was decreased markedly (Figure 3i). Next, through an analysis of the differences in the species composition of the gut microbiota, we observed substantial disparities in the relative abundance of gut microbiota among the top 15 species within the model group, with an increase of 7 species (*Escherichia_coli_g__Escherichia-Shigella*, *Lactobacillus_murinus*, uncultured*_bacterium_g__Ruminococcus_torques_group*, uncultured*_bacterium_g__Turicibacter*, *Romboutsia_ilealis*, *Bacteroides_thetaiotaomicron* and *Bifidobacterium_pseudolongum*) and a decrease of 8 species (uncultured*_bacterium_g__norank_f__Muribaculaceae*, unclassified *_g__norank_f__norank_o__Clostridia*_UCG-014, uncultured*_bacterium_g__Prevotellaceae*_UCG-001, uncultured*_bacterium_g__Prevotellaceae*_NK3B31*_group*, uncultured*_bacterium_g__Lachnospiraceae*_NK4A136_group, unclassified*_f__Lachnospiraceae*, uncultured*_Bacteroidales_bacterium_g__norank_f__Muribaculaceae* and uncultured*_Clostridiales_bacterium_g__ Lachnospiraceae*_NK4A136_group). Nevertheless, after intervention with *L. acidophilus* treatment, it was observed that only a significant decrease in *E.coli_g__Escherichia-Shigella* was observed, while a significant increase in fourteen other species was observed compared to the model group. Further, there was a significant elevation in the abundance of ten types of bacteria after ASA treatment compared with the DSS group. Evidently, the relative abundance of all 15 species in the DSS-AS group was significantly different than that in the DSS-LA group. Two species (*Lactobacillus_murinus* and unclassified*_g__Enterococcus*) in the DSS-AS group were noticeably increased, whereas the others were considerably decreased. Ultimately, we can see that the regulatory effect of *L. acidophilus* on DSS-induced intestinal microbiota disturbance is evidently superior to that of ASA (Figure 3j).

In order to analyze the interactions between these bacterial species, a bacterial network was constructed. Network analysis revealed that uncultured_*bacterium_g__norank_f__Muribaculaceae*, unclassified_*g__norank_f__norank_o__Clostridia*_UCG-014, uncultured_*bacterium_g__Ruminococcus_torques_group*, *E.coli_g__Escherichia-Shigella*, uncultured_*bacterium_g__Prevotellaceae*_UCG-001, uncultured_*bacterium_g__Erysipelatoclostrium* and *Romboutsia lealis* may play the crucial roles in interactions (Figure 4a). Meanwhile, Circos map analysis shown that some beneficial bacteria such as uncultured_*bacterium_g__norank_f__Muribaculaceae*, uncultured_*bacterium_g__Prevotellaceae*_UCG-001 and uncultured_*bacterium_g__Ruminococcus_torques_group*, were most prevalent in the DSS-LA group (Figure 4b).

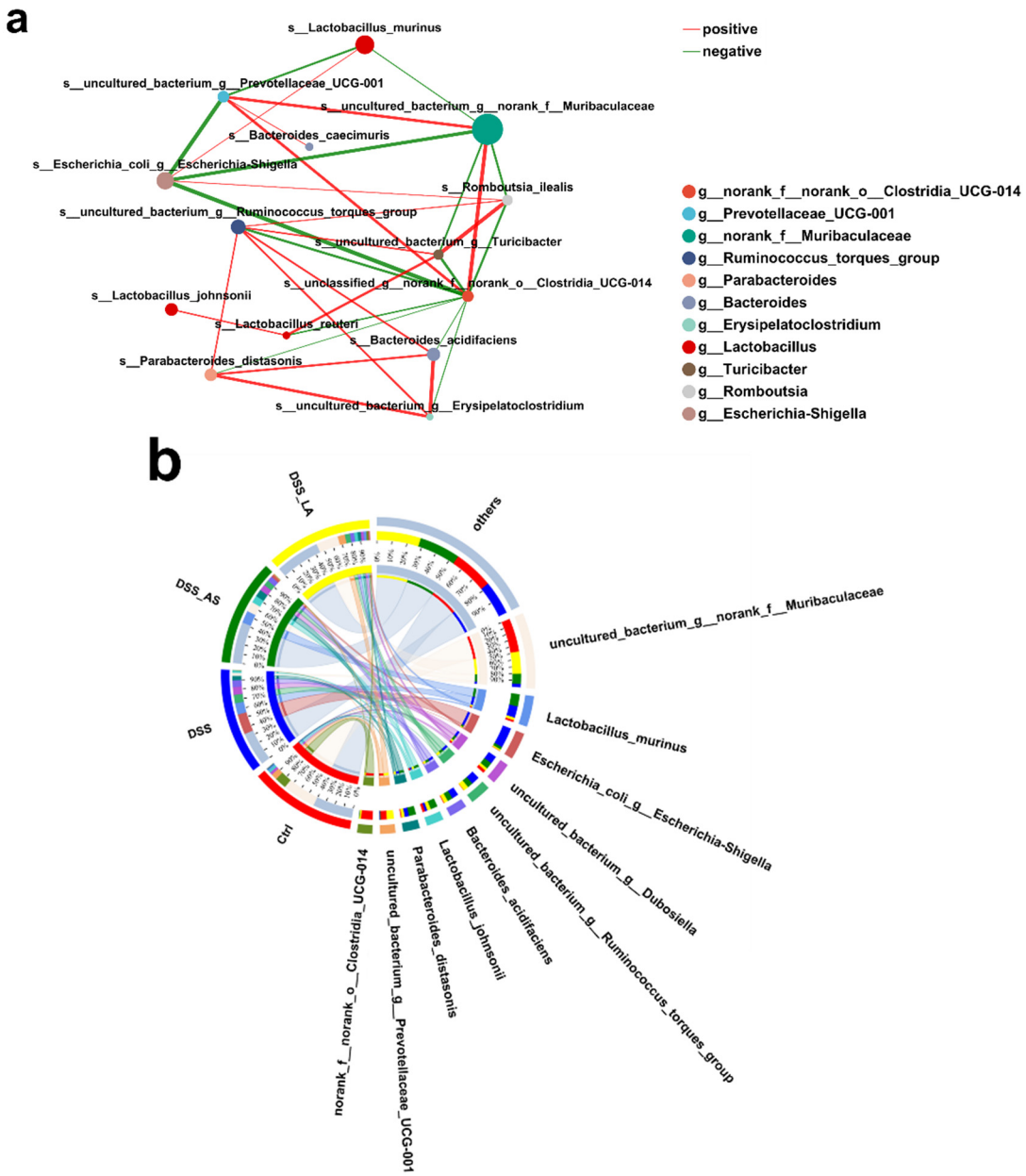

Figure 4 (a) Species correlation network diagram of each group. Analyzed by Spearman rank correlation analysis. The size of the circle represents the average abundance of the species; the line represents the correlation between the two species; the thickness of the line represents the strength of the correlation; and regarding the color of the line, red represents a positive correlation, and green represents a negative correlation; (b) Circos map visualizing the most abundant classes in the Ctrl, DSS, DSS-AS, and DSS-LA; Others combined the relative abundance of classes <0.01.

In addition, Linear discriminant analysis (LDA) effect size method (LEfSe) was employed to further investigate the distinct bacterial community structure among the Control group, DSS group, DSS-AS group and DSS-LA group (Supplementary Figure 3a and b). According to the results, there were prominent differences in the abundance of different levels of taxa in the four groups. In particular, Bacteroidota, Bacteroidia, Bacteroidales, Clostridia_UCG-014, Oscillospirales, norank_o__Clostridia_UCG-014, Muribaculaceae, Prevotellaceae, *Lachnospiraceae*_NK4A136_group, *norank_f__Muribaculaceae*, unclassified*_f__Lachnospiraceae*, *norank_f__norank_o__Clostridia*_UCG-014, unclassified*_f__Lachnospiraceae*, unclassified *_g__norank_f__norank_o__Clostridia*_UCG-014, uncultured*_Bacteroidales_bacterium_g__norank_f__Muribaculaceae* uncultured*_bacterium_g__Lachnospiraceae*_NK4A136_group and uncultured*_bacterium_g__norank_f__Muribaculaceae* played an essential role in the Ctrl group and could be used as biomarkers, Whereas Proteobacteria, Actinobacteria, Gammaproteobacteria, Bifidobacteriales, Enterobacterales, Bifibacteriaceae, Enterobacteriaceae, *Escherichia-Shigella, Bifidobacterium, Ruminococcus_torques_group, Bacteroides_thetaiotaomicron*, *E.coli_g__Escherichia_Shigella*, *Bifidobacterium_pseudolongum* and *uncuitured_bacterium_g__Ruminococcus_torques_group* were indispensable and could serve as a biomarker in the DSS group. Further, Bacilli, Erysipelotrichales, Lactobacillales, Peptostreptococcales-Tissierellales, Lactobacillaceae, Peptostreptococcaceae, Tannerellaceae, *Lactobacillus*, *Parabacteroides*, *Romboutsia*, *Turicibacter*, *Lactobacillus_murinus*, *Lactobacillus_reuteri*, *Romboutsia_ilealis*, *Parabacteroides_distasonis,* uncultured*_bacterium_g__Erysipelatoclostridium*, uncultured*_bacterium_g__Turicibacter* and functioned importantly and could be taken as a biomarker in the DSS-AS group, as well as Bacteroidaceae, Bacteroides, Prevotellaceae_UCG-001, norank_f__Lachnospiraceae, *Bacteroides_caecimuris*, unclassified*_g__norank_f__Lachnospiraceae*, uncultured *_bacterium_g__Prevotellaceae*-UCG-001 played a crucial part and could be employed as a biomarker in the DSS-LA group. Obviously, the DSS group exhibited a higher number of taxa with differential abundance compared to the DSS-LA group, indicating that *L. acidophilus* treatment exerts a restorative effect on specific microbiota alterations in the DSS-induced colitis model. Last but not least, the *L. acidophilus* intervention for one week exhibited a positive impact on enhancing the diversity of the gut microbiota, thereby suggesting its potential in regulating intestinal microbiota homeostasis.

3.3.3. Effects of L. acidophilus supplement on the gut microbiota function

As the second-largest genome in the human body, the intestinal microbiota plays a crucial role in maintaining growth, development, and overall health. Consequently, they have garnered significant attention due to their physiological functions within the host organism (55, 56). Moreover, studies have demonstrated dysregulation of gut microbiota in UC mice, specifically characterized by alterations in potential metabolic, immune-related, and disease-associated functions. These changes in microbial physiology may potentially contribute to the onset of UC (27, 54). Therefore, PICRUSt was conducted to predict the functional potential

of bacteria, and subsequent analysis was carried out in the context of the Kyoto Encyclopedia of Genes and Genomes (KEGG) database. As depicted in Figure 5a and Supplementary Figure 4a-e, the enzyme, ORTHOLOGY (KO), modules, pathways and COG function classification belonging to KEGG functional categories were identified. Moreover, the DSS group exhibited six significantly distinct functional categories compared to the Ctrl group. However, these differences were largely mitigated by the *L. acidophilus* intervention. To sum up, the *L. acidophilus* intervention ameliorates gut microbiota functions related to inflammatory injury, metabolism, immune response, and pathopoiesia.

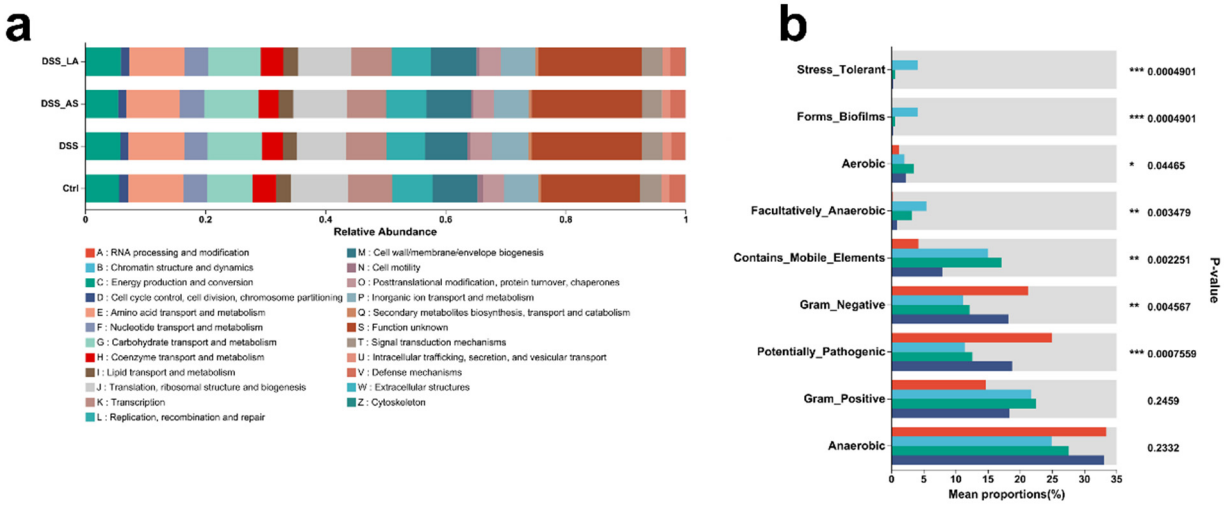

Figure 5 Effects of *L. acidophilus* on intestinal microbiota function and phentype. microbiota function basing Kyoto Encyclopedia of Genes and Genomes (KEGG) database in colitis mice. Effects of probiotics *L. acidophilus* treatment on (a) COG function classification; (b) Effects of *L. acidophilus* on gut microbiota phenotype basing BugBase including Stress_Tolerant, Forms_Biofilms, Aerobic, Facultatively_Anaerobic, Contains_Mobile_Elements, Gram Negative, Potentially_Pathogenic, Gram Positive, and Anaerobic. ns > 0.05; * $P < 0.05$; * * $P < 0.01$ and * ** $P < 0.001$ versus Ctrl; & $P < 0.05$, && $P < 0.01$ and &&& $P < 0.001$ versus DSS; # $P < 0.05$, ## $P < 0.01$ and ### $P < 0.001$ versus DSS-LA.

3.3.4. Effects of L. acidophilus supplement on the gut microbiota phenotype

The nine potential microbial phenotypes including Stress_Tolerant, Forms_Biofilms, Aerobic, Facultatively_Anaerobic, Contains_Mobile_Elements, Gram Negative, Potentially_Pathogenic, Gram Positive, and Anaerobic ones were analyzed by the BugBase to predict the organism-level coverage of functional pathways and biointerpretable phenotypes of bacteria (Figure 5b and Supplementary Figure 4f). Notably, the relative abundance of Contains_Mobile_Elements, Facultatively_Anaerobic, Forms_Biofilms, and Stress_Tolerant in the DSS group was significantly increased compared to that in the Ctrl group. Conversely, there was a remarkable decrease in the abundance of Gram-negative and Potentially_Pathogenic phenotypes. This data deviate from previous literature reports possibly due to a substantial reduction in beneficial Gram-negative bacteria such as *norank_f__Muribaculaceae*, *Prevotellaceae*_UCG-001, Candidatus saccharimonas and Alistipes within the DSS model group (Supplementary Figure 4g). Additionally, a significant increase in harmful bacteria including Bacteroides, Parabacteroides, Parasutterella, and Escherichia-Shigella was observed in the DSS model group; however, a significant decrease in several potential bacteria like *norank_f__Muribaculaceae*, *norank_f__norank_o__Clostridia*_UCG-014, Alistipes and *Prevotellaceae*_UCG-001 that may be beneficial for maintain body health. This increase was relatively

minor compared to the decrease mentioned above resulting in lower levels of Potentially_Pathogenic phenotypes within DSS the model group when compared to the control (Supplementary Figure 4g). Intriguingly, the *L. acidophilus* treatment had a significant regulatory effect on some specific microbiota phenotypes that can make the phenotype in a beneficial direction in the DSS group (Supplementary Figure 4f and g).

3.4 L. acidophilus restored immune imbalance in colitis mice

Previous studies have indicated that immune system dysfunction, including an imbalance of Th1 cells, Th2 cells, Th17 cells, and Treg cells along with the cytokines they secrete, is considered a major contributor to UC (57, 58). To investigate whether *L. acidophilus* play a crucial role in regulating T cell activation and differentiation in UC mice, splenocytes from different groups were collected and analyzed using flow cytometry. The results demonstrated that compared to the normal group, there was an increase in the percentage of Th17 cells in the spleen of the model group mice while there was a decrease in the percentage of Th2 and Treg cells. However, intervention with *L. acidophilus* effectively mitigated these effects. Moreover, it is well-established that both Th17 and Treg cells are important components for maintaining immune balance alongside Th1 and Th2 cells. Imbalances between these subsets are believed to contribute to various autoimmune and inflammatory diseases (59, 60). In consequently, we observed an evident imbalance between expression levels of Th1/Th2 as well as Th17/Treg cells in the DSS group where upregulated levels of both Th1 and TH17 were accompanied by downregulated levels of both Th2 and Treg when compared to control group, while supplement *L. acidophilus* could somewhat mitigated this influences (Figure 6a).

An increasing number of studies have reported that immune and inflammatory pathways of the intestinal epithelial barrier serve a critical role in the initiation and progression of UC, and inflammatory cytokines can significantly modulate the disease progression of UC (61). In our study, we assessed the immune status in vivo by detecting the expression of 11 cytokine profiles in blood samples by ELISA. As compared with the control group, the expression levels of 9 cytokines after oral administration of DSS for 8 days were significantly up-regulated, including IL-4, IL-6, IL-18, IL-17, TNF-α, IL-1β, IL-22, IL-23, and IL-10, After 16 days, the pro-inflammatory cytokines IL-4, TNF-α, IL-10 were dramatically reduced in the colon tissue of colitis mice after the *L. acidophilus*, while the expression levels of IL-17, IFN-γ, MPO and IL-1β were notably up-regulated (Figure 6b–l). These data manifested that the administration of *L. acidophilus* supplements results in significant changes to the cytokine profile in mice with DSS-induced colitis, suggesting that its palliation effect on UC may be attributed to the modulation of specific inflammatory mediators.

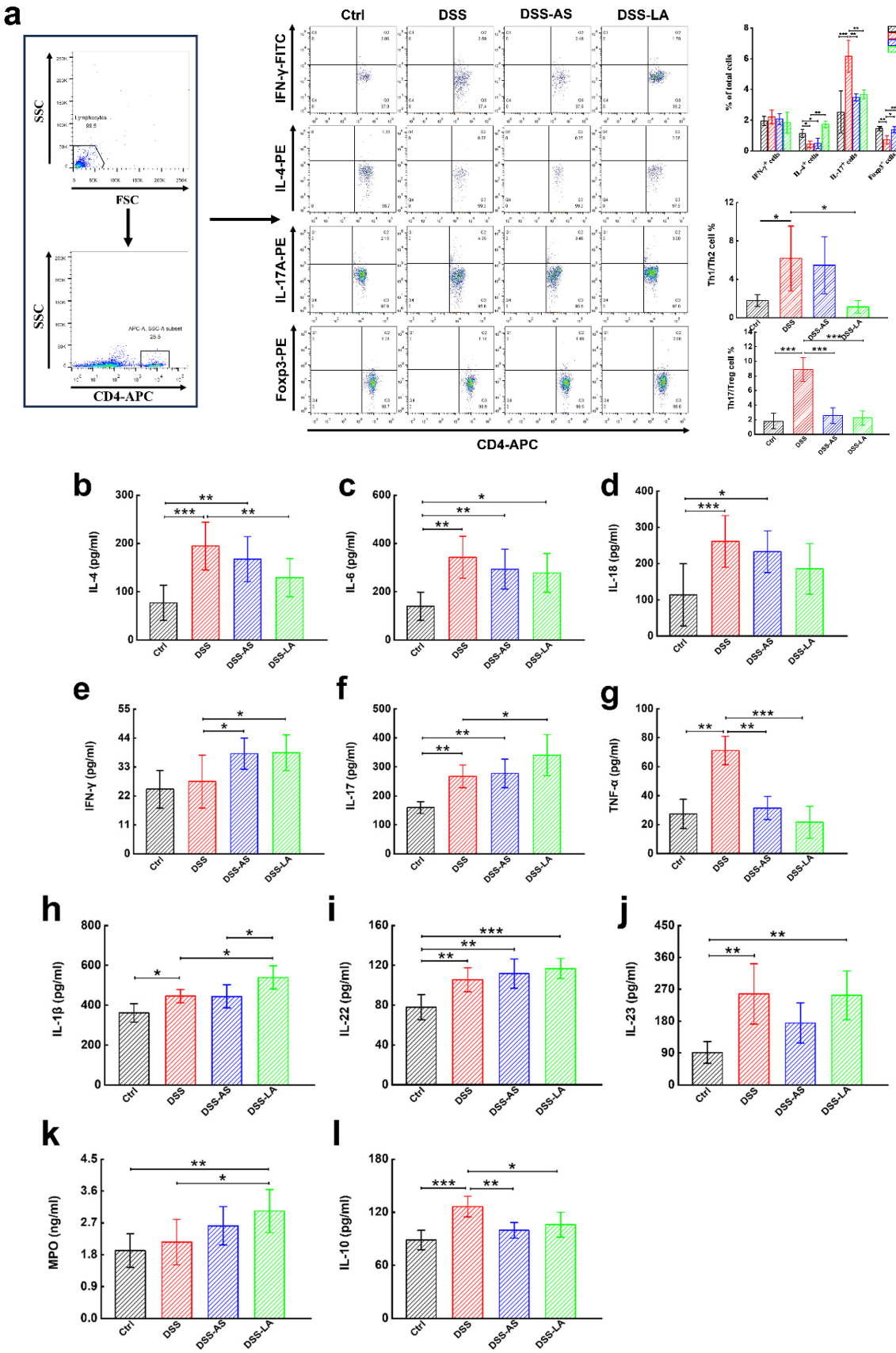

Figure 6. Effects of *L. acidophilus* on immune imbalance in colitis mice. (a) Single cells were isolated from the spleens, counted, and stained with cell markers to identify Th1, Th2, Th17 and Treg cells. Typical CD4$^+$IFN-γ^+ Th1 cells, CD4$^+$IL-4$^+$ Th2 cells, CD4$^+$IL17A$^+$ Th17 cells and CD4$^+$Foxp3$^+$ Treg cells flow cytometry were shown, calculation of the percentage of Th1, Th2, Th17, Treg cells to the total number of CD4 + cells, and the percentage of Th1/Th2 cell and Th17/Treg cell. The expression of (b) IL-4, (c) Il-6, (d) IL-18, (e) IFN-γ, (f) IL-17, (g) TNF-α, (h) IL-1β, (i) IL-22, (j) IL-23, (k) MPO and (l) IL-10 were assessed in serum by ELISA. Data were showed as mean ± SD (n = 7). ns > 0.05; * $P < 0.05$; ** $P < 0.01$; *** $P < 0.001$.

3.5 L. acidophilus regulated Th17/Treg Balance and maintained the mucosal immune in colitis mice

In immune homeostasis, the gut contains very few CD4 T cells, and only contains scattered interepithelial lymphocytes and inherent lymphocytes of the intestinal mucosal epithelium (62). However, the presence of increased CD4T cell content or normal CD4T cell number in the intestinal mucosal epithelium, but showing increased activation and phenotypic changes, maybe a potential mechanism for the development of UC (63-66). Among them, T cell-mediated adaptive immune response can cause the activation of neutrophils, macrophages and other immune cells, and aggravate intestinal mucosal inflammation, so it plays an important role in the pathogenesis of UC (67, 68). Hence, phenotypic analyses of T cells in lamina propria and epithelial cells (LPCs) of colitis mice were performed by flow cytometry. The results suggested that, although the supplementation of *L. acidophilus* had no significant effect on the DSS-changed proportion of Th2 cells, the level of Th1 cells and Th17 cells was distinctly down-regulated and the number of Treg cells was significantly up-regulated (Figure 7). Simultaneously, it is noteworthy that the *L. acidophilus* demonstrates a prominent capacity to restore the balance of Th17/Treg and Th1/Th2. The results suggest that the improvement of colitis by *L. acidophilus* may be related to the restoration of intestinal immune homeostasis of Th17/Treg and Th1/Th2 in DSS-induced colitis mice.

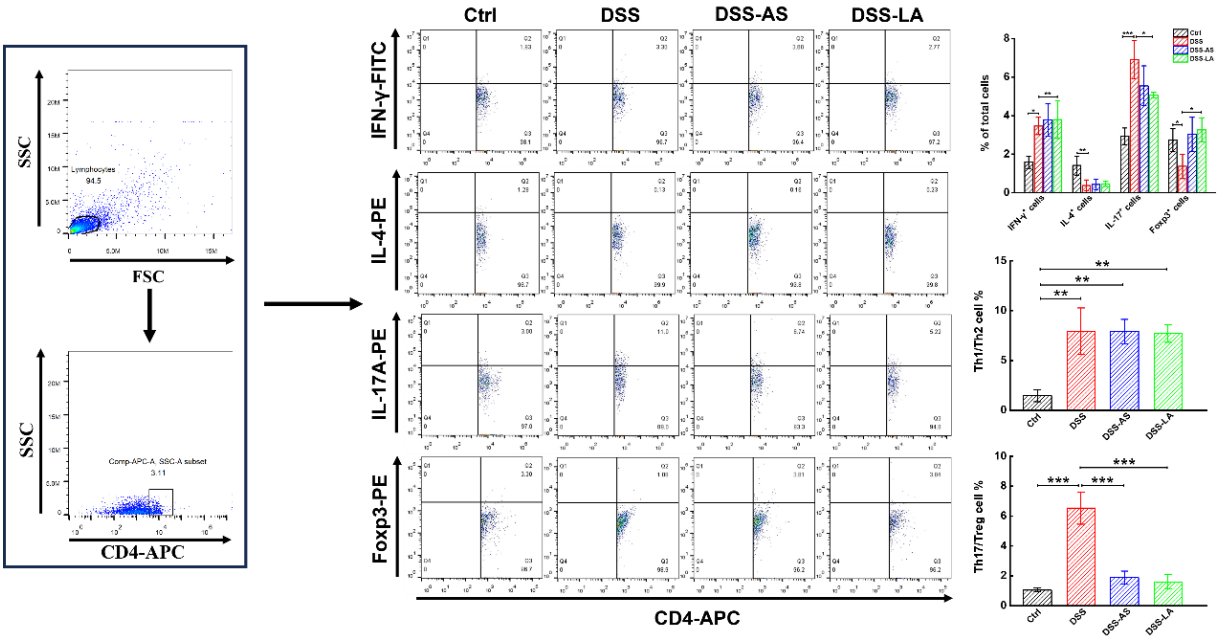

Figure 7. Effects of *L. acidophilus* on colonic mucosal immune imbalance in colitis mice. Percentages of Th1 cells, Th2 cells, Th17 cells and Treg cells in colonic LPCs were detected by using flow cytometry assay. Percentage of T-cell subpopulations gated on CD4+ T cells, and ratio of Th1/Th2 and Th17/Treg cells. Data were showed as mean ± SD (n = 7). ns > 0.05; * $P < 0.05$; ** $P < 0.01$; *** $P < 0.001$.

3.6 L. acidophilus may resisted the oxidative stress by regulating the Nrf2/NF-κB signaling pathways in colitis mice

Compelling evidence suggests that oxidative stress and inflammatory response, represented by the nuclear transcription factor Nrf2 and NF-κB signaling pathways respectively, are absolutely correlated and have a highly cross-linked process that simultaneously play a crucial role in inflammatory diseases (69, 70). With this in mind, we not only analyzed the expressions of oxidative stress-related proteins (SOD, GSH-Px,

MDA) in the colon tissues of mice in each group, but also examined the effect of the *L. acidophilus* on Nrf2 and NF-κB signaling pathway protein expression in mouse colon tissue by immunohistochemistry and western blot, respectively. In agreement with previous studies (56), the DSS challenge caused a decrease in the activities of GSH-Px while increased after *L. acidophilus* intervention. It is regrettable that SOD and MDA had changed but did not reach the statistically significant level (Figure 8a). Furthermore, as shown in Figure 8b, as compared with the control group, the expression of nuclear Nrf2 was markedly down-regulated and Keap-1 was up-regulated acutely in the colon tissues of mice by DSS administration, and these effects were eliminated by the *L. acidophilus* rather than ASA, suggesting that the *L. acidophilus* may alleviate colitis by unblocking the inhibitory effect of DSS on the antioxidation signaling pathway.

At the same time, given that UC leads to rapid activation of the NF-kB signaling pathway, which leads to the production of a large number of pro-inflammatory factors, we investigated the effects of *L. acidophilus* or ASA treatment on this pathway in colon tissue. As anticipated, compared with the control group, serum LPS level and TLR4 protein levels, NF-κB P65 and I-κB phosphorylated protein levels were relatively elevated in the model group (Figure 8c), indicating that DSS induces an inflammatory cascade through activation of the NF-kB pathway, which was attenuated by *L. acidophilus* or ASA supplementation. These findings suggest that the ameliorative effect of *L. acidophilus* supplementation on colitis may be attributed to activation of the Nrf2 antioxidative signaling pathway and inhibition of the NF-κB inflammatory signaling pathway.

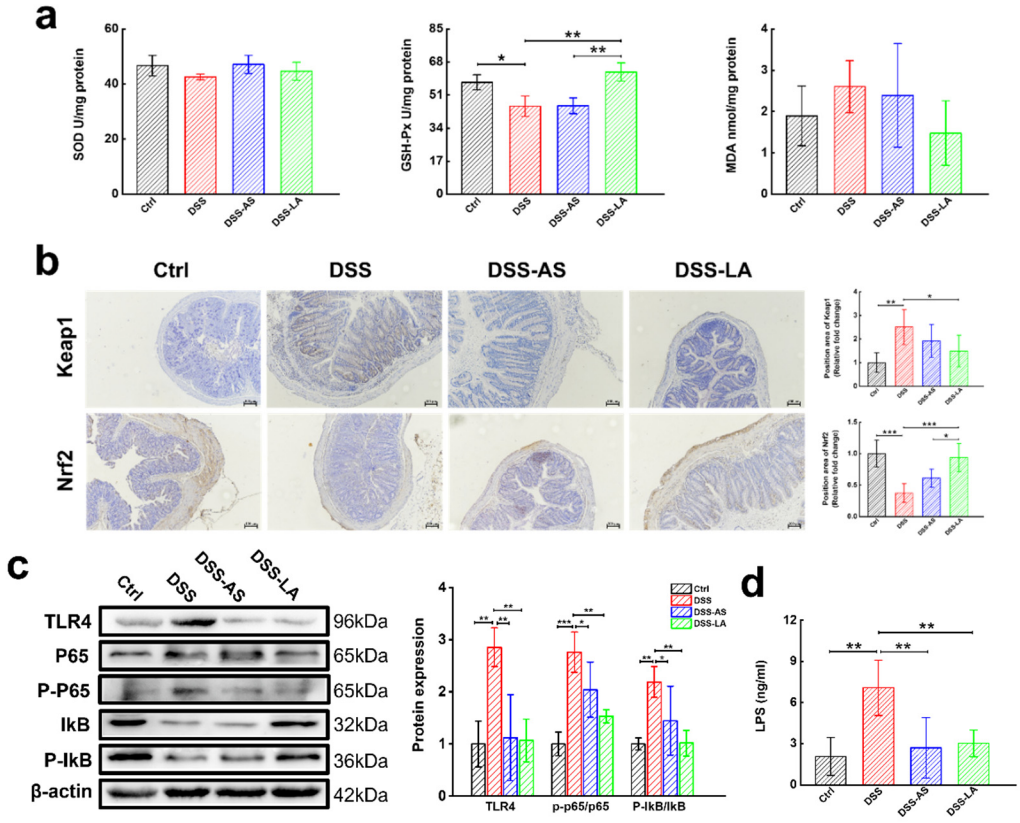

Figure 8. *L. acidophilus* regulated antioxidative and inflammatory signaling pathways in colitis mice. (a) The expression of SOD, GSH-Px, and MDA were assessed in colon tissue by ELISA; (b) Immunohistochemistry staining and quantitative analysis of Nrf2 and Keap-1 proteins in colon tissues from different treatment groups, Scale bar = 100 μm; (c) Representative immunoblots and the relative expression levels of TLR4, P65, P-P65, IkB and P-IkB proteins in colon tissues from different treatment groups; (d) serum LPS level. Data were showed as mean ± SD (n = 7). ns > 0.05; * $P < 0.05$; ** $P < 0.01$; *** $P < 0.001$.

3.7 L. acidophilus alleviated UC via pathways involving Gut Microbiota-BAs-FXR/FGF15 signaling

Some studies have pointed out that BAs, as pleiotropic signaling metabolites, are closely related to intestinal microbiota and its metabolites, and disruption of bile acid homeostasis can accelerate the pathological process of colitis (71, 72). Therefore, in order to explore how the *L. acidophilus* affects bile acid homeostasis in enterohepatic circulation, we preliminarily investigated the expression of bile acid-related FXR/FGF15 signaling pathway protein in the liver and ileum of colitis mice. Firstly, BAs primarily circulate in the liver-gut system, and their regulation through the FXR/FGF15 pathway ultimately takes place in the liver. Therefore, we observed the appearance of mouse livers and found that there was no significant difference between the four groups (Supplementary Figure 5a). Then, HE staining and oil red O staining were performed on the livers to evaluate its pathological characteristics. We observed that treatment with *L. acidophilus* or ASA was effective in reducing inflammation and lipid deposition in the liver cells of mice with colitis (Figure 9a, Supplementary Figure 5b). Subsequently, the results indicated a significant increase in FXR and CYP7A1 mRNA levels in the livers of model group compared to those in the normal group. Following *L. acidophilus* intervention, there was a dramatic decrease in these levels. Consistently, the ileal CYP7A1 mRNA level in DSS group was significantly higher than that in normal group, and the FXR mRNA level was also increased, but the difference was not significant, and there was no significant change in either of them after *L. acidophilus* intervention. (Figure 9b). Meanwhile, it was noted that the expression of FXR and FGF15 proteins was significantly elevated while CYP7A1 expression was notably decreased in the livers of DSS-treated mice compared to those in the Control group. Following administration of *L. acidophilus*, there was a significant reduction in FXR and FGF15 protein expression along with an increase in CYP7A1 protein expression. Although the content of FXR and FGF15 decreased significantly after ASA treatment, the expression of CYP7A1 protein did not increase evidently (Figure 9c). Besides, we also evaluated the expression of FXR and FGF15 proteins in the ileum (Figure 9d). Compared to expression in the Control group, the expression of FXR and FGF15 was clearly upregulated in the DSS group of mice, and significantly downregulated after the administration of *L. acidophilus*. Nevertheless, the expression level of FXR in ASA group mice did not change markedly. Altogether, these data suggest that the *L. acidophilus* may influence BA synthesis by modulating FXR-FGF15 signaling pathways in liver and ileum, thereby improving UC in mice.

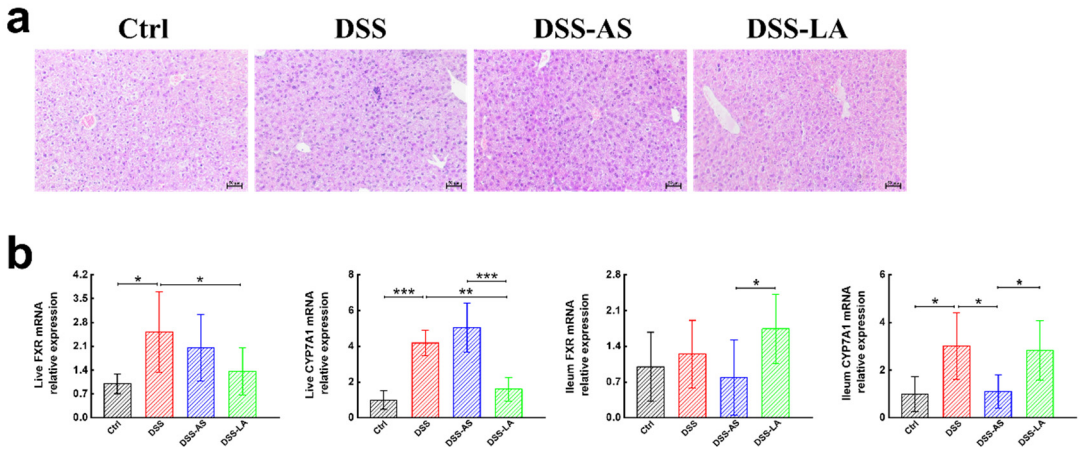

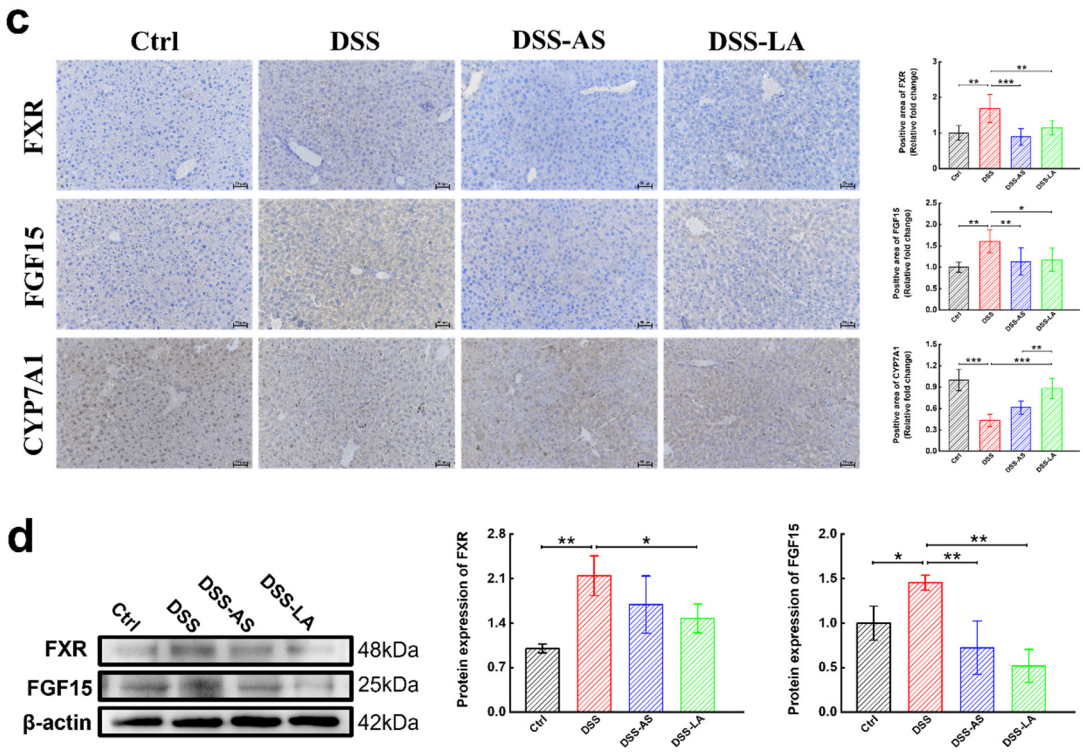

Figure 9. *L. acidophilus* regulated FXR/FGF15 signaling pathways in colitis mice. (a) Photographs of HE-stained sections of livers, Scale bar = 50 μm; (b) The mRNA levels of FXR, and CYP7A1 for each group in the liver and ileum; (c) Immunohistochemistry staining and quantitative analysis of FXR, FGF15 and CYP7A1proteins in liver tissues from different treatment groups. (d) Representative immunoblots and the relative expression levels of FXR and FGF15 proteins in ileum tissues from different treatment groups. Data were showed as mean ± SD (n = 7). ns > 0.05; * $P < 0.05$; ** $P < 0.01$; *** $P < 0.001$ group.

3.8 L. acidophilus improved UC by Inhibiting the activation of NLRP3 Inflammasome and reducing pyroptosis

The nucleotide-binding domain-like receptor family pyrin domain containing 3 (NLRP3) is a prototypical inflammasome that may be involved in the pathogenesis of various inflammatory diseases (73). Studies have demonstrated that NLRP3-deficient mice exhibited reduced susceptibility to DSS-induced acute colitis, highlighting the essential role of the NLRP3 inflammasome in UC pathogenesis (74). Recent investigations have revealed that Gin Rg3 inhibited NLRP3 inflammasome activation and pyroptosis, leading to the amelioration of UC symptoms in mice (28). To ascertain whether the therapeutic effect of *L. acidophilus* on UC mice involves modulation of NLRP3 inflammasome activity, we assessed the expression levels of pyroptosis-related indicators in the colon of UC mice. Immunohistochemistry results indicated that DSS treatment elevated the expression levels of NLRP3, ASC, pro-Caspase-1, Caspase-1 and GSDMD-N (Figure 10a and b), as well as increased serum concentrations of IL-18 and IL-1β (Figure 6d and h). However, *L. acidophilus* intervention reversed these DSS induced effects to varying degrees. These findings align with a recent study conducted by Dai et al. (75), who assessed the impact of *Bacillus paralicheniformis* HMPM220325 on DSS-induced UC in mice, as evidenced by marked downregulation of IL-1β and IL-18 mRNA levels, and expression levels of NLRP3 inflammasome-associated proteins or genes in colonic tissue compared to the DSS group.

Unexpectedly, after *L. acidophilus* treatment, serum levels of IL-1β were significantly higher than those in the model group; additionally, there was an increase in serum IL-18 level compared to that in the model group without reaching statistical significance. Overall, these results suggest that *L. acidophilus* effectively alleviate DSS-induced UC in mice through potential inhibition of NLRP3 inflammasome activation and pyroptosis.

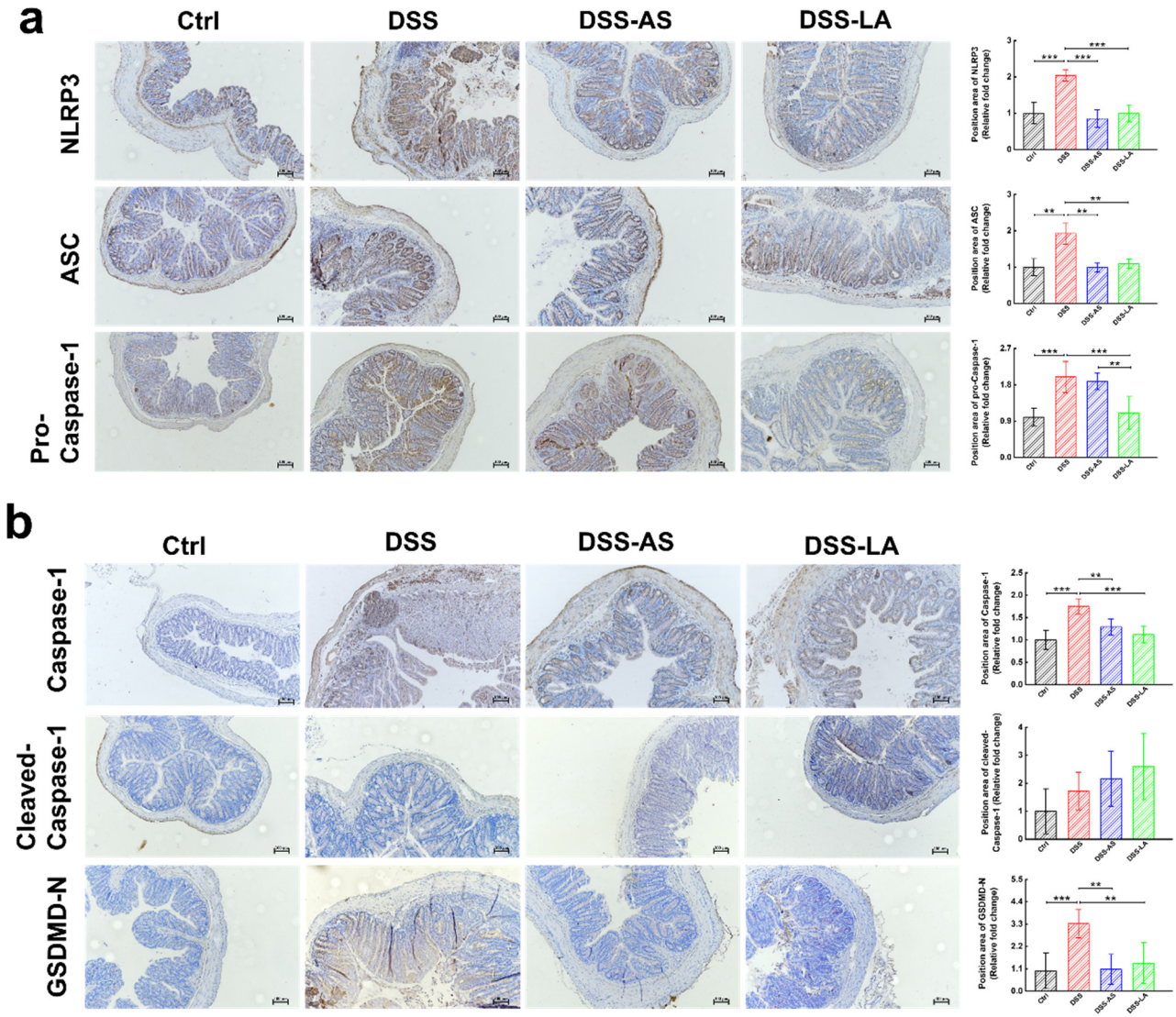

Figure 10. *L. acidophilus* inhibited NLRP3 inflammasome activation in colitis mice. (a) Immunohistochemistry staining and quantitative analysis of NLRP3, ASC and pro-Caspase-1 protein content in the distal colon, Scale bar = 100 μm; (b) Immunohistochemistry staining and quantitative analysis of Caspase-1, cleaved-Caspase-1 and GSDMD-N protein content in the distal colon (scale bar, 100 um). Data were showed as mean ± SD (n = 7). ns > 0.05; * $P < 0.05$; ** $P < 0.01$; *** $P < 0.001$ group

3.9 Correlation analysis of gut microbiota, body weight, colon length, bacterial translocation, intestinal barrier function, inflammation response and BAs metabolism

Using Mantel Test network heat map analyses, the correlations between clinical factors (colitis index, colon TJPs, serum inflammatory factors levels, bacterial translocation, colon immune cells differentiation, inflammatory response, and bile acid regulation) and microbial community structure at species level demonstrated that gut microbiota species played an important role in maintaining gut barrier function, regulating inflammation, oxidative stress, pyroptosis, and bile acid metabolism immune regulation and bile

acid metabolism (Figure 11a). Moreover, from heatmap correlation analysis, it is seen that in the 15 top species, 15 species were notably associated with these clinical factors (Figure 11b). uncultured_bacterium_g__*Erysipelatoclostridium*, E.coli_g__*Escherichia-Shigella*, uncultured_bacterium_g__*Turicibacter*, *Romboutsia_ilealis*, *Parabacteroides_distasonis*, uncultured_bacterium_g__*Ruminococcus*_torques_group, *Lactobacillus_murinus* were obviously and positively correlated with serum inflammatory factors, colon Th1 cells and Th17 immune cells proportion, colonic TLR4/NF-κB-related proteins expression as well as colon pyroptosis related proteins expression, but noticeably negatively correlated with colitis index, colon TJPs mRNA expression, colon Th2 cells and Treg immune cells proportion, colon oxidative stress and liver CYP7A1 proteins expression (Figure 11b). Thus, these bacterial species may induce UC development. In addition, uncultured_bacterium_g__*Prevotellaceae*_UCG-001, unclassified_g__norank_f__norank_o__*Clostridia*_UCG-014, uncultured_bacterium_g__ norank_f__*Muribaculaceae* were observably correlated with serum inflammatory factors, the proportion of Th1 cells and Th17 immune cells in the colon, colonic TLR4/NF-κB-related proteins expression and colon pyroptosis related proteins expression in a negative way, but positively correlated with colitis index, colon TJPs mRNA expression, colon Th2 cells and Treg immune cells proportion, colon oxidative stress as well as liver CYP7A1 proteins expression in an obvious manner (Figure 11b). Thus, these bacterial species may alleviate UC.

To further study the interactions between the top 15 species with clinical factors, we constructed a species and factors correlation network map. Then, network analyses revealed that the 9 species play an important role in regulating clinical factors. Details are as follows: unclassified_*g__norank_f__norank_o__Clostridia*_UCG-014, uncultured_*bacterium_g__norank_f__Muribaculaceae*, *E.coli_g__Escherichia-Shigella* and uncultured_*bacterium_g__Ruminococcus*_torques_group are most closely related to these clinical factors and may be the essential player in *L. acidophilus* mitigation of UC. In particular, unclassified_*g__norank_f__norank_o__Clostridia*_UCG-014 was strongly positively correlated with body weight and occludin gene expression, while significantly negatively correlated with IL-4, IL-6, IL-18, IL-23, pp65/p65, GSDMD-N, lamina propria Th1 cells and Th17 cells. uncultured_bacterium_g__ norank_f__*Muribaculaceae* is significantly positively correlated with body weight, ZO-1 and occludin mRNA expression, and negatively correlated with liver FGF15, GSDMD-N and PP65/P65 expression. From this, it can be seen that these two bacteria both contribute to the recovery of UC. On the contrary, uncultured_bacterium_g__*Ruminococcus*_torques_group also plays an important role in the development of colitis. It was positively correlated with IL-17, IL-18, PP65/P65, lamina propria Th1 cells and Th17 cells, and strongly negatively correlated with body weight and formation of lamina propria Th2 cells. Along the same lines, E.coli_g__*Escherichia-Shigella* was strongly positively correlated with inflammatory cytokines IL-6, IL-18, lamina propria Th17 cells and pp65/p65, while strongly negatively correlated with body weight; these

results suggest that uncultured_bacterium_g__*Ruminococcus*_torques_group and E. coli may be a potential strain to promote the progression of UC (Figure 11c). All in all, these findings demonstrated that the 9 bacterial species play vital roles in colitis development.

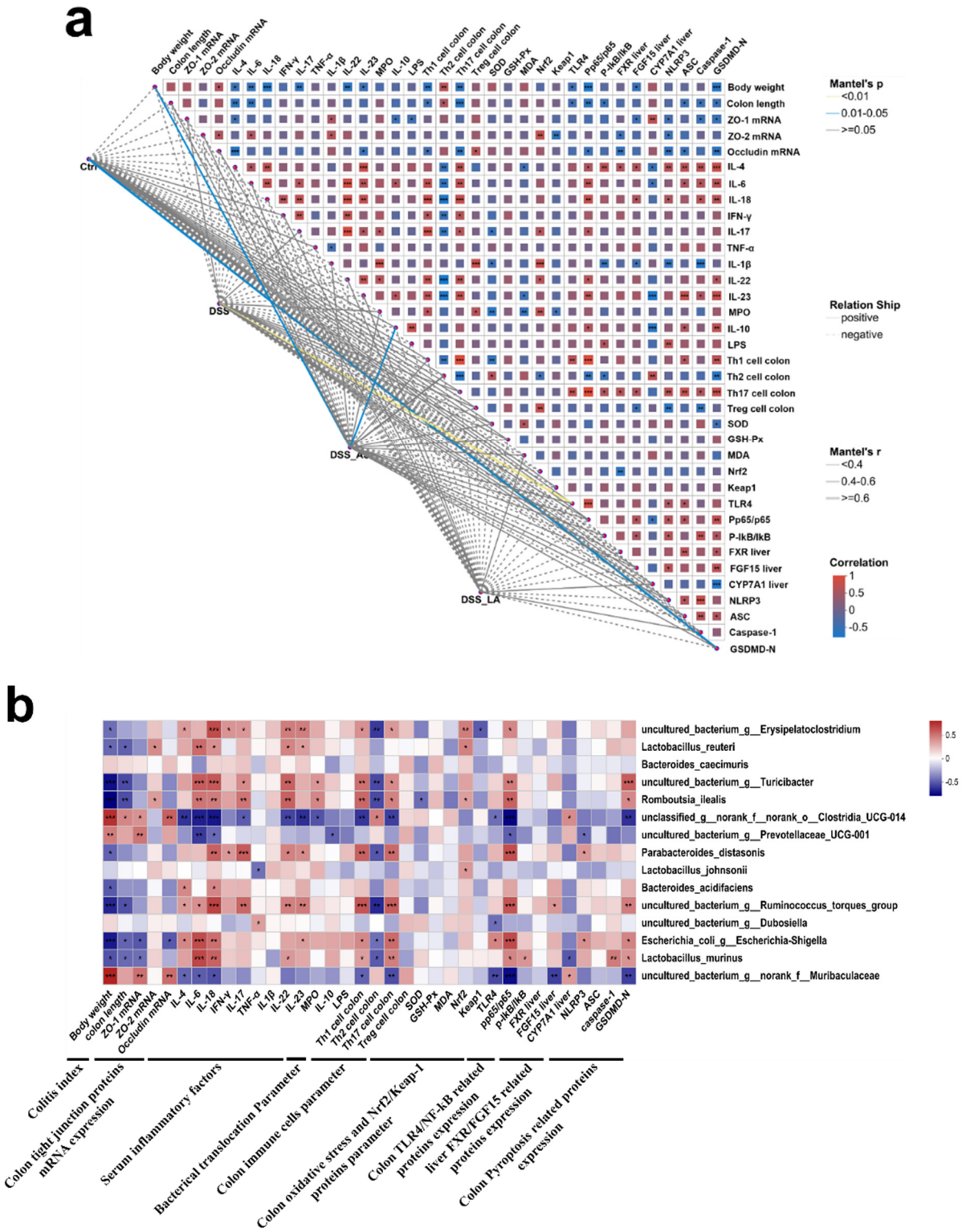

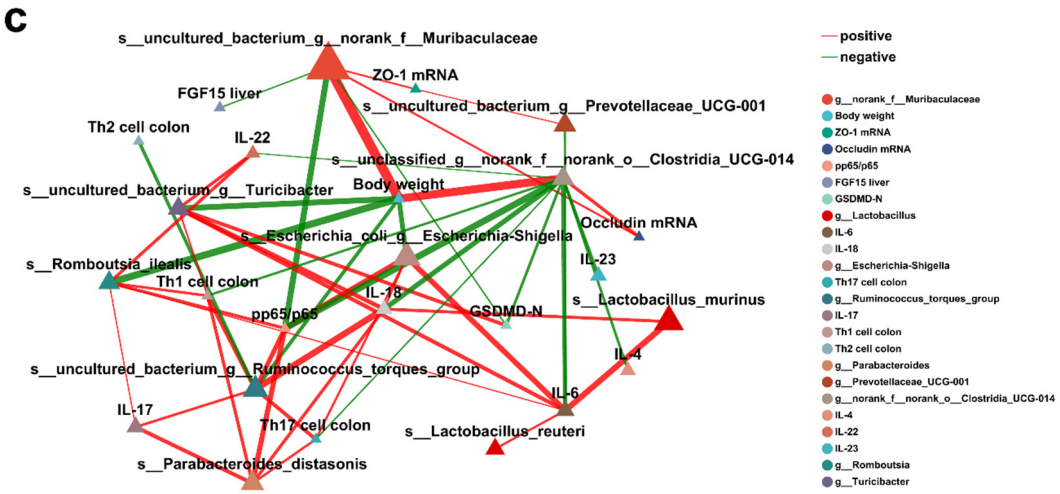

Figure 11. (a) Variations of gut microbiota species and clinical factors have obvious relationship in the Ctrl, DSS, DSS-AS, and DSS-LA. The correlation between clinical factors and microbial community structure was evaluated by Mantel Test network heat map analysis analyze. The lines represent the correlation between gut microbiota species and clinical factors, and the heat map represents the correlation between clinical factors; the thickness of the line represents the strength of the correlation, * $0.01 < P \leq 0.05$, ** $0.001 < P \leq 0.01$, *** $P \leq 0.001$. (b) The relationship between clinical factors (body weight, colon length, intestinal barrier function, degree of bacterial translocation, inflammatory response, Nrf2/NF-kB/NLRP3 pathway and bile acid regulatory pathway FXR/FGF15) and the 15 top species is estimated by Spearman's correlation analysis. *, $P < 0.05$; **, $P < 0.01$; ***, $P < 0.001$. (c) Network maps between gut microbiota species and clinical factors were analyzed by Spearman rank correlation analysis ($P \leq 0.05$). The size of nodes represents the average abundance of the species or factors, and different colors represent different species or factors. The line represents the correlation between the two species. The thickness of the line indicates the size of the correlation coefficient, and the thicker the line, the higher the correlation between species. The more lines, the closer the connection between the nodes. The color of the line indicates positive and negative correlation, red indicates positive correlation, green indicates negative correlation.

4. Discussion

Currently, many probiotics, especially *L. acidophilus*, has been proven to effectively alleviate UC by regulating intestinal flora, strengthening intestinal wall function and regulating immune imbalances (76). Consistent with previous studies (25, 28, 77, 78), our discovered that *L. acidophilus* administration not only obviously attenuated the severity of colitis in mice, including reducing weight loss, DAI scores, organ index and histological scores while increasing food intake, water consumption and colonic length; it also mitigated various pathological injuries such as sparse and shortened microvilli, expanded intercellular space, severe mucosal damage, loss of goblet cells, deformation of crypts and hyper-infiltration of neutrophils in comparison to the DSS group. Furthermore, *L. acidophilus* showed favorable anti-inflammatory effects by regulating the gut microbiota composition and maintaining the intestinal barrier integrity. Interestingly, *L. acidophilus* was somewhat superior to 5-ASA in restoring the gut microecology and improving intestinal functions, which was an important driver of UC symptom improvement. In conclusion, our results indicate that *L. acidophilus* is able to effectively relieve DSS induced UC mice by regulating the gut microbiota, intestinal barrier function and inflammation.

UC is globally recognized for its high prevalence that is characterized by a chronic dysregulation of the inflammatory response in the gastrointestinal tract (79). Notably, the precise of the initiation and/or propagation of the inflammation for UC is still unknown and is difficult to remove, however it is believed to have a multifactorial etiology. Intestinal permeability increase and Intestinal flora disturbance lead to harmful substances such as bacteria and LPS into the blood, stimulate lymphocyte differentiation and related

inflammatory factors secretion, and trigger various inflammatory reactions. Looking at it in reverse, the excessive release of inflammatory cytokines plays a pivotal role in the destruction of the intestinal barrier, which further contributes to the development of inflammation (80). This inflammatory cascade leads to a continuous disruption of the intestinal barrier, fueling the chronic and progressive nature of the disease (7).

It is well known that damage to the structure and function of the intestinal mucosal barrier is closely related to the occurrence and development of UC (17, 81). Intestinal permeability serves as an indicator for assessing the intestinal barrier integrity and safeguarding the epithelium from detrimental factors (82, 83). Goblet cells play a pivotal role in defending the intestinal mucosal barrier by secreting mucus proteins to counteract the invasion of harmful substances (84). Intriguingly, histological analysis showed that *L. acidophilus* and ASA supplementation both prevented neutrophil infiltration, increased the number of goblet cells and crypts, restored intestinal epithelial permeability and injury. Similarly, TJPs effectively regulate paracellular transport to prevent bacteria, toxins, and other substances from entering the blood, thereby maintaining the integrity of epithelial barrier function in the intestinal mucosa. However, DSS treatment significantly reduces TJPs expression leading to increased intestinal permeability, bacterial translocation, elevated serum FITC-dextran levels and endotoxin concentration which further exacerbate inflammatory response. In this study, *L. acidophilus* intervention can upregulate ZO-1, ZO-2 and Occludin expression, restore colonic TJs, thus positively impacting the maintenance of structural integrity to prevent colitis occurrence.

Intestinal flora disturbance in patients with UC and in animals is associated with a decrease in flora diversity, especially a significant decrease in beneficial bacteria (85, 86), demonstrating that the gut microbiota plays a pivotal role in the pathogenesis of UC. Probiotics feeding reverses the trend of declining diversity and effectively improves the symptoms of colitis (87-89), and our study observed that *L. acidophilus* treatment the DSS-treated mice effectively improved the alpha diversity and changed the community composition. Specific manifestation is as follows: at the phylum level, the dominant bacterial groups in each group were Bacteroidetes, Firmicutes, Proteobacteria, and Actinobacteria, which accounted for over 97% of taxonomy general. Specifically, the Firmicutes to Bacteroidetes ratio and the abundance of Firmicutes and Proteobacteria in the model group were significantly higher but were close to the normal group after *L. acidophilus* intervention, which are consistent with the results of a recent study conducted by Ridaura et al.(32). Moreover, the abundance of the phylum Actinobacteriota was strongly associated with the activity of intestinal inflammatory diseases (90) and its abundance was significantly reduced after *L. acidophilus* supplementation.

At the genus level, the *L. acidophilus* changed the structure of intestinal bacteria via increasing the abundance of beneficial bacteria, such as *norank_f__norank_o__Clostridia*_UCG-014, *Prevotellaceae*_UCG-001, *Lachnospiraceae*_NK4A136_group, norank_f__Muribaculaceae and unclassified_f__Lachnospiraceae, and reduceing the abundance of harmful bacteria, such as norank_f__Lachnospiraceae and *Escherichia-Shigella*. The genus

*norank_f__norank_o__Clostridia*_UCG-014 demonstrates resilience to gastric acid, promotes beneficial bacteria growth, inhibits harmful intestinal tract growth, restores intestinal flora, improves immunity, and facilitates nutrient absorption and digestion (26). Similarly, *Prevotellaceae* UCG-001, a gram-negative obligate anaerobic bacillus, has the capacity to ferment carbohydrates and produce SCFAs such as acetate and butyrate, exerting an anti-inflammatory effect on immune cells and suppressing potentially invasive pathogenic bacteria (91, 92). Additionally, *Lachnospiraceae*_NK4A136_group is recognized as a significant butyrate producer that maintains immune homeostasis by regulating Th17/Treg balance (93, 94). As the potentially beneficial bacterium, unclassified_f__Lachnospiraceae has the ability to produce SCFAs and regulate cholesterol metabolism (95, 96), while the role of norank_f_Muribaculaceae in host physiology remains unclear, studies suggest its potential positive impact on attenuating oxazolone-induced colitis severity in mice through improvement of intestinal mucositis (97). These reports support the possibility that *L. acidophilus* may help maintain intestinal microenvironment stability by assisting these probiotics mentioned above colonize, thereby reducing DSS induced intestinal inflammation. On the contrary, the norank_f__Lachnospiraceae has been reported to be positively associated with levels of inflammation and oxidative stress (98). The *Escherichia-Shigella*, a representative genus of Aspergillus, is an LPS-producing Gram-negative bacteria. This not only compromises Th17/Treg conversion and intestinal immune homeostasis but also can adhere to colonic mucosal epithelial cells and correlates with increased pro-inflammatory cytokine expression, ultimately leading to impaired intestinal barrier integrity (99, 100). Therefore, these two types of bacteria are likely key pathogenic agents contributing to the development of UC, which aligns with previous findings (13, 71).

At the species level, likewise, Our results revealed that augmentation of uncultured*_bacterium_g__norank_f_Muribaculaceae*, uncultured*_Bacteroidales_bacterium_g__norank_f_Muribaculaceae* and uncultured*_bacterium_g__Prevotellaceae* UCG-001 along with reduction of *E.coli_g__Escherichia-Shigella* potentially mediated the protective effects of the *L. acidophilus* treatment on UC. The uncultured*_bacterum_g_norank_f_muribaculaceae* and uncultured*_Bacteroidales_bacterium_g__norank_f_Muribaculaceae* have been identified as the possible target microorganisms in the occurrence of colitis, which can inhibit the pathogenic bacteria growth and intestinal colonization by occupying ecological space (101, 102). Additionally, it was noted that uncultured*_bacterium_g__ Prevotellaceae* UCG-001 is an advantageous bacterium that was found to enhance microbial fermentation and facilitate the conversion of polysaccharides into SCFAs and prevent colitis (103). These results manifest that the impact of supplementation with *L. acidophilus* may be at least partly due to the increase in the population of these beneficial species and reduce several types of bacteria associated with inflammation and intestinal barrier disruption. Therefore, *L. acidophilus* treatment can relieve UC by adjusting the composition of the intestinal microbiota and their metabolites in a variety of ways.

At the onset of UC, intestinal immune homeostasis is significantly compromised, shown by immune cell infiltration into colonic mucosa and release of inflammatory mediators, which drive UC progression through positive feedback mechanisms (104-106). It is noteworthy that Th1 cells can modulate intestinal inflammation and prevent pathogen invasion through secretion of TNF-α and IFN -γ to stimulate innate immune cell activation (107, 108), and elevated levels of these factors observed in UC mice support an association with exacerbated Th1 immune responses and intestinal inflammation. Intriguingly, *L. acidophilus* intervention reduced the production of Th1 cells and TNF-α to varying degrees, while increasing IFN-γ production. As is well-known, TNF-α promotes intraepithelial cell apoptosis and inflammation, whereas IFN -γ stimulates macrophages and neutrophils recruitment by inducing adhesion molecule expression on intraepithelial cells (109, 110), but it is now documented that Th17 and Treg cells can also produce IFN-γ (111). Appropriate secretion of IL-1β not only regulates the expression of TJPs and restores intestinal barrier function, but also enhances the phagocytic capacity of mononuclear phagocytes and plays a pivotal role in the pyroptosis process with IL-18 to maintain intestinal immune homeostasis (112-115). This may explain the significant increase in IL-1β observed following the administration of *L. acidophilus*.

Up-regulation of Th2-related cytokines such as IL-4, IL-6 and IL-10 promotes humoral immune responses along with mucosal IgA response occurrence (84, 116), and upregulation of Th17 cells in peripheral blood of UC patients was accompanied by elevated levels of several key inflammatory factors such as IL-17, IL-22, and IL-23, which was positively correlated with disease activity (117). Critically, IL-17 modulates intestinal barrier function and induces the release of inflammatory chemokines and cytokines from target cells (121), while IL-22 activates the proliferation of intestinal stem cells and promotes tissue regeneration, thereby preserving the integrity of intestinal epithelial cells (118, 119). consistent with elevated levels of IL-22 in both the model and probiotic treatment groups in this study. Consequently, these data suggest that L. acidophilus has the potential to regulate the intestinal mucosal immune response, which is beneficial for the enhancement of host defense mechanisms. Furthermore, Treg cells can inhibit intestinal inflammation caused by abnormal immune responses of autoantigens and symbiotic bacteria and play an essential role in suppressing immune responses and maintaining peripheral tolerance and immune homeostasis (120). Likewise, Treg cells in the lamina propria of the colon specifically express the transcription factor Foxp3, effectively inhibiting autoimmunity and preventing tissue damage by secreting the anti-inflammatory factor IL-10 (117, 121). In our experiments, *L. acidophilus* effectively inhibited the expression of IL-4, TNF-α, IL-10, and corresponding with remarkerly augment the expression of IFN-γ, IL-17 and IL-1β through various mechanisms, thereby exerting its anti-inflammatory effects. These mechanisms include the regulation of Th1/Th2 and Th17/Treg balance (71, 122, 123), modulation of bile acid metabolic homeostasis (124), regulation of NLRP3 inflammasomes and pyroptosis (125) and inhibition of Nrf2/NF-κB signal transduction (87).

In addition, it has been reported that MPO, a heme protein, is the main component of neutrophils, as a key mediator of the innate immune system, neutrophils are rapidly recruited to sites of inflammation, where they recognize, phagocytose, and inactivate foreign microbes (126). In addition, MPO plays a vital role in

controlling and terminating the phagocytosis activity of neutrophils, and its oxidants are also involved in inhibiting the function of lymphocytes. These properties make MPO beneficial for maintaining tissue homeostasis (127), which is consistent with elevated MPO levels observed in colon tissue from the DSS-LA group. Therefore, it is acknowledged that the *L. acidophilus* supplement may enhance the intestinal self-defense capability, regulate the body's immune dynamic balance, and ultimately alleviate the severity of colitis.

In general, Nrf2 and NF-κB are inseparable during anti-inflammatory and antioxidative processes (128). Under inflammation conditions, activation of IκB kinase (IKK) results in phosphorylation-mediated degradation release of IκB, leading to nuclear translocation and activation of NF-κB which upregulates inflammatory cytokine gene expression and induces production of oxygen free radicals causing tissue damage (129). Similarly, under conditions of oxidative stress, dissociation of Nrf2 from Keap1 allows it to translocate into the nucleus where it binds to antioxidant response elements (ARE), activating antioxidative enzymes such as SOD,CAT and GSH-Px (130). As a major ligand of TLR4, LPS from Gram-negative bacteria can cause severe inflammatory damage and even death by activating the TLR4/NF-κB p65 inflammatory signaling pathway (131). In this study, the serum LPS level was noticeably reduced after the intervention of *L. acidophilus* or ASA. At the same time, it is mainly due to the fact that *L. acidophilus* prevents LPS from entering the bloodstream from the intestine by improving the intestinal barrier function. Moreover, elevated inflammatory factors TNF-α, IL-6, and IL-1β also promote Keap1 transcription and expression, strengthening Nrf2 inhibition and degradation, thereby exacerbating UC symptoms (132, 133), which elucidates why Keap1 expression is upregulated in the DSS group while it decreases after the intervention with *L. acidophilus*.

Additionally, Keap1 promotes degradation release of IκK thereby enhancing stability of IκB which inhibits activation of NF-κB signaling pathway and competition between NF-κB p65 and Nrf2 for binding to CBP modulates transcriptional activity. However, overexpressed p65 will preferentially bind to CBP, inhibiting the transcriptional activity of Nrf2, leading to increased inflammation and oxidative stress(134). Previous investigators treating UC with olmesartan or licochalcone A involved activating the Nrf2 signaling pathway and inhibiting the NF-κB signaling pathway (130, 135). Inversely, $Nrf2^{-/-}$ mice showed stronger signs of NF-κB activation following inflammatory stimulation compared to wild type mice (136), and Nrf2-regulated antioxidant enzymes such as SOD have been demonstrated to regulate NF-κB signal transduction (137), and in our study the antioxidant enzymes SOD and GSH-Px were also increased. Clearly, modulating aberrant NF-κB and Nrf2 signaling pathways and maintaining their homeostasis may represent an effective therapeutic approach for UC, and our data suggest that the effective protective effects of *L. acidophilus* are likely to be a universal benefit through reducing oxidative damage and inflammation.

Recent reports suggest that the disturbance of bile acid metabolism could play a significant role in driving the progression of UC (138). Theoretically, conjugated BAs function as endogenous antagonists for FXR, while unconjugated BAs act as agonists for the FXR-FGF15 feedback pathway (139). In the liver, activated FXR induces the expression of SHP, which subsequently binds to LRH-1 and indirectly inhibits the

expression of CYP7A1 (140). In the ileum, activated FXR upregulates FGF15 expression, which enters the enterohepatic circulation and binds with FGFR4 mediated by β-KLOTHO to downregulate CYP7A1 expression (141, 142). In this study, the expression of FXR and FGF15 in the liver increased in DSS group mice and decreased after *L. acidophilus* administration, and *L. acidophilus* intervention vastly decreased DSS-induced increases in hepatic mRNA levels for both FXR and CYP7A1. In the ileum, although the expression of FXR and CYP7A1 mRNA was not significantly changed by *L. acidophilus* treatment, the changes in FXR and FGF15 expression induced by DSS were significantly reversed, ultimately leading to an increase in liver CYP7A1 expression and bile acid synthesis. However, these results are contrary to previous findings, and we speculate that the likely cause is that the increase in unbound BAs induced by self-metabolic compensations in UC mice activates the bile acid regulatory pathway FXR/FGF15, which in turn inhibits the activity of CYP7A1, which is mitigated by *L. acidophilus* treatment (143, 144). In conclusion, these results manifest that *L. acidophilus* can regulate the FXR/FGF15 signaling pathway maintaining bile acid homeostasis within enterohepatic circulation improving metabolism thus alleviating UC symptoms.

Pyroptosis, a new form of programmed cell death, has been widely studied in inflammatory disease models in recent years (145). The successfully assembled NLRP3 inflammasome is a key regulator of pyroptosis and its upregulated expression can promote the development of inflammation (52). NLRP3 inflammasome consists of NLRP3, ASC, and pro-caspase-1 (146). Upon the activation of NLRP3, ASC and Caspase-1 are recruited. Subsequently, activated NLRP3 and ASC facilitate pro-caspase-1 dimerization and Caspase-1 activation, which activates and divides GSDMD, resulting in a GSDMD-N terminal fragments that further bind to cell membranes and perforate, triggering cell pyroptosis and promoting the secretion and release of IL-1β and IL-18 (147, 148). Further, NLRP3$^{(-/-)}$ mice-induced DSS developed less severe colitis than wild-type mice and produced lower levels of proinflammatory cytokines in colonic tissue (149). Evidence showed that Live *L. acidophilus* has already been confirmed to improve UC mice by inhibiting the NLRP3 inflammasome activation (37). Consistent with previous research, we indeed observed that *L. acidophilus* could suppress pyroptosis by down-regulating the expressions of NLRP3, ASC, pro-Caspase-1, Caspase-1 and GSDMD-N, indicating the anti-colitis effects of *L. acidophilus* in this research. Therefore, the inactivation state of the NLRP3 inflammasome could serve as a potential target to ameliorate UC. In addition, the intervention of *L. acidophilus* resulted in a reduction of serum IL-18 levels compared to the model group, although this difference did not reach statistical significance, and there was a significant increase in IL-1β content, which may be attributed to the involvement of multiple regulatory pathways of cytokines. Intriguingly, a recent study conducted by Ridaura et al. used JSH-23, the inhibitor of NF-κB p65, to prove that NF-κB controlled NLRP3 and pyroptosis in inflammatory bowel disease (150, 151). This is consistent with the results we discussed above that *L. acidophilus* exerts anti-inflammatory effects by inhibiting the activation of the NF-κB signaling pathway, thereby alleviating UC. Consequently, our data suggest that the inhibition of the NLRP3 inflammasome and pyroptosis activation may mediate the protective effect of *L. acidophilus* against DSS-induced colitis.

Last but not least, this study revealed significant differences in the microbiome phenotypes and bacterial functional potential among the four groups of mice. The BugBase analysis discovered a prominent reduction in potentially pathogenic traits such as Stress_Tolerant and Forms_Biofilms following *L. acidophilus* treatment. Additionally, predicted bacterial KEGG functional profiles by PICRUSt manifested higher relative abundance of energy metabolism, inflammatory response, and pathopoiesia across all groups, suggesting their significant advantages, while *L. acidophilus* treatment restored these functions to levels comparable to those observed in normal mice. Simultaneously, supplementation with *L. acidophilus* alters the composition and function of the bacteria in the "gut microbiota organ." Within this context, it is reasonable to speculate that these changes in composition and function may establish a reciprocal relationship between members of the "new" microbiome, metabolites, and the host immune system, which contributes to the recovery of intestinal dysbiosis.

On the basis of the above, our work illustrated that *L. acidophilus* showed a effective amelioration effect on colitis mice, and its mechanism may be related to preserve intestinal barrier function integrity, modulate microbial homeostasis, inhibit the TLR4/NF-κB, NLRP3/Caspase-1, and Nrf2/Keap1 signaling pathway, as well maintain the balance of bile acid metabolism. In addition, microbiome phenotype prediction and bacterial functional potential prediction analysis demonstrated that the *L. acidophilus* supplementation regulated gut microbiota function involving inflammatory injury, metabolism, immune response, and pathopoiesia. Conspicuously, the *L. acidophilus* not only optimized microbial composition directly by enhancing beneficial microbes and reducing potentially harmful bacteria but only rebuilt immune system homeostasis by restoring the balance of Th1/Th2 cells as well as Th17/Treg cells along with specific inflammatory cytokine expression, in order to achieve improvement in the complex symptoms of UC. Additionally, although *L. acidophilus* demonstrated comparable efficacy to mesalazine in this study, clinical observations revealed a marked increase in fecal mucus among mice treated with mesalazine, sometimes accompanied by symptoms such as diarrhea and vomiting. Besides, molecular experiments showed that mesalazine exhibited weaker efficacy in intestinal barrier repair and microbiota regulation compared to *L. acidophilus* in UC mice. Above all, these parameters indicate that this neoteric *L. acidophilus* possesses the advantages of anti-inflammatory, antioxidant, anti-pyroptosis, regulates bile acid metabolism, promotes the repair of intestinal epithelial damage and the restoration of intestinal homeostasis, highlighting its significant potential as a probiotic for the treatment of colitis. Therefore, it may serve as a promising candidate for the treatment of UC without side effects.

5. Conclusion

Taken together, this study provides compelling evidence that newly *L. acidophilus*, isolated from the porcine intestines, not only enhances intestinal barrier integrity, and reshapes microbial composition but also reduces colonic inflammation, inhibits pyroptosis, significantly mitigates oxidative stress damage. Consequently, it effectively reverses colon damage and restores function in mice with UC. Thus, the potential mechanism may involve the restoration immune balance, inhibition pyroptosis activation and regulation bile

acid metabolism, and is associated with the Nrf2/NF-κB/NLRP3 signal transducing pathways and the FXR-FGF15 feedback pathway (Figure 12). More importantly, our data indicated that the new *L. acidophilus* was as effective in treating UC as mesalazine but without the side effects. Consequently, the great potential of probiotics *L. acidophilus* to alleviate UC will provide promising clinical treatment strategies and greatly broaden the application prospect of UC in clinical treatment

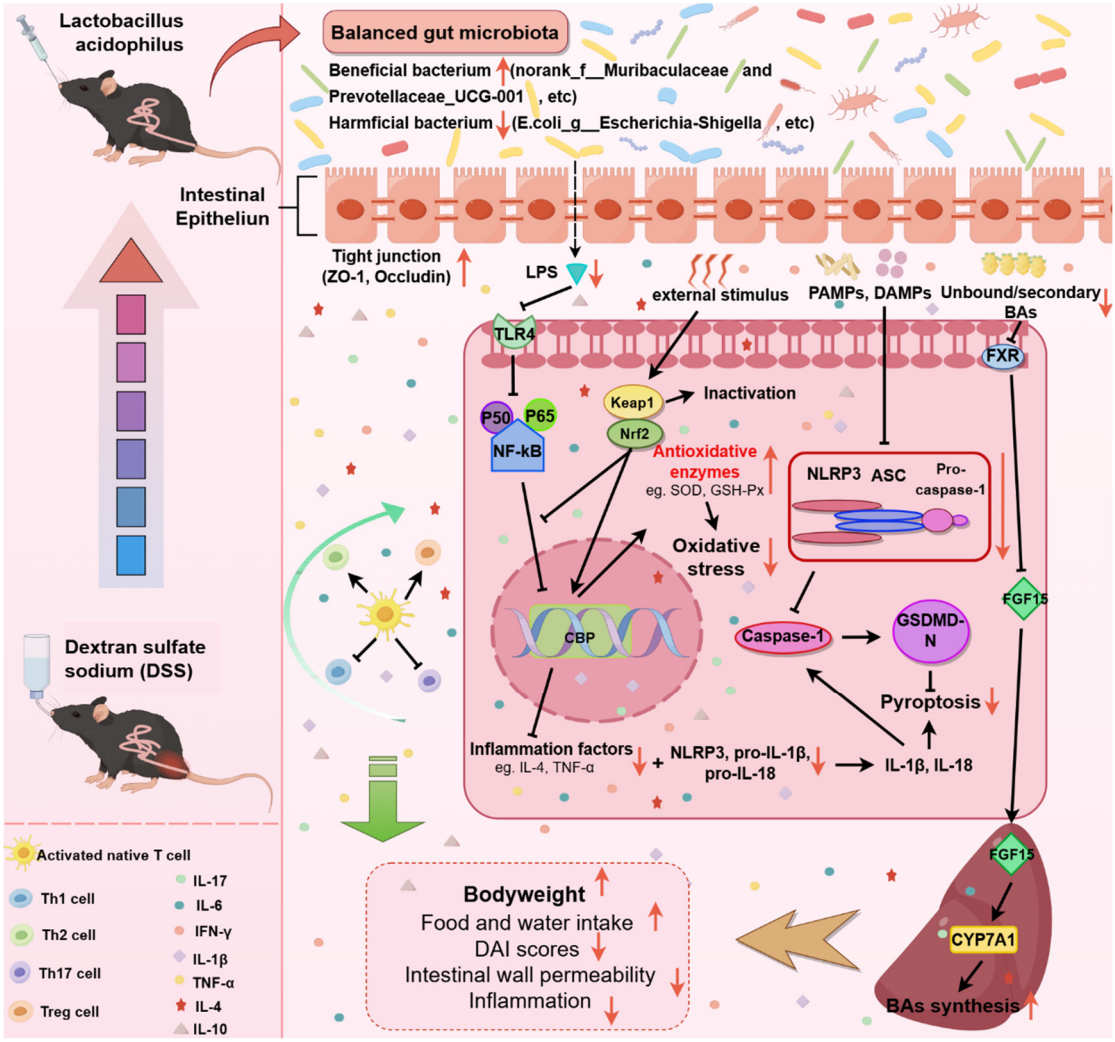

Figure 12. The mechanisms underlying the protective effects of novel *L. acidophilus* against DSS-induced colonic inflammation in mice are illustrated in a schematic representation. Administration of *L. acidophilus* resulted in significant remission in DSS-induced UC models. Firstly, *L. acidophilus* treatment preserved the intestinal microbial equilibrium by enhancing the abundance of beneficial bacteria while concurrently diminishing harmful bacterial populations. Secondly, *L. acidophilus* gavage improved intestinal architecture and reduced permeability through upregulation of TJPs, thereby preventing translocation of intestinal bacteria and endotoxins into the bloodstream, which could trigger immune responses. Thirdly, *L. acidophilus* significantly downregulated Th1/Th2 and Th17/Treg ratios, effectively modulating inflammatory cytokine levels to maintain immune homeostasis within the body, particularly in the intestinal epithelium, and mitigating oxidative stress damage; this may involve modulation of Nrf2/NF-kB signaling pathways. Notably, it also inhibited NLRP3 inflammasome assembly to suppress pyroptosis and reduce inflammation further. Additionally, *L. acidophilus* may reduce the level of unbound or secondary bile acid levels, inhibit the activation of the FXR/FGF15 signaling pathways within hepatointestinal circulation, ultimately regulating bile acid metabolism and inflammatory states. Collectively, these findings underscore that probiotic *L. acidophilus* plays a pivotal role in restoring gut microbial balance, enhancing intestinal barrier function, attenuating inflammatory responses, pyroptosis and oxidative stress damage while regulating bile acid metabolism.

Acknowledgements

Not applicable.

Funding

This work was supported by Shanxi Province Natural Science Foundation (Grant No. 202203021221182), Science Research Start-up Fund for Doctor of Shanxi Medical University (Grant No. XD1807), Science Research Start-up Fund for Doctor of Shanxi Province (Grant No. SD1807), Scientific and Technological Innovation Programs of Higher Education Institutions in Shanxi (Grant No. 2019L0425), and Shanxi Province Higher Education "Billion Project" Science and Technology Guidance Project (Grant No. BYJL045).

Availability of data and materials

The data that support the findings of this study are available from the corresponding author, upon reasonable request.

Declaration of interests

The authors declare that they have no known competing financial interests or personal relationships that could have appeared to influence the work reported in this paper.

Reference

1. Neumann H, Kiesslich R. Endomicroscopy and endocytoscopy in IBD. Gastrointestinal endoscopy clinics of North America. 2013;23(3):695-705.
2. Khor B, Gardet A, Xavier R. Genetics and pathogenesis of inflammatory bowel disease. Nature. 2011;474(7351):307-17.
3. undefined u, undefined u, undefined u, undefined u, undefined u, undefined u. Dihydroberberine, an isoquinoline alkaloid, exhibits protective effect against dextran sulfate sodium-induced ulcerative colitis in mice. Phytomedicine. 2021;90.
4. undefined u, undefined u, undefined u, undefined u, undefined u, undefined u, et al. Worldwide incidence and prevalence of inflammatory bowel disease in the 21st century: a systematic review of population-based studies. Lancet. 2017;390.
5. Jiahui Z, Huan L, Pei Z, Shijun Y, Bingtao Z, Junbo Z, et al. Paeonol Ameliorates Ulcerative Colitis in Mice by Modulating the Gut Microbiota and Metabolites. Metabolites. 2022;12(10).
6. Zheng K, Zhang S, Wang C, Zhao W, Shen H. Health-related quality of life in Chinese patients with mild and moderately active ulcerative colitis. PloS one. 2015;10(4):e0124211.
7. Chen Y, Liang J, Chen S, Lin N, Xu S, Miao J, et al. Discovery of vitexin as a novel VDR agonist that mitigates the transition from chronic intestinal inflammation to colorectal cancer. Molecular cancer. 2024;23(1):196.
8. Ungaro R, Mehandru S, Allen P, Peyrin-Biroulet L, Colombel J. Ulcerative colitis. Lancet (London, England). 2017;389(10080):1756-70.
9. Yu YR, Rodriguez JR. Clinical presentation of Crohn's, ulcerative colitis, and indeterminate colitis: Symptoms, extraintestinal manifestations, and disease phenotypes. Seminars in pediatric surgery. 2017;26(6):349-55.
10. da Silva BC, Lyra AC, Rocha R, Santana GO. Epidemiology, demographic characteristics and prognostic predictors of ulcerative colitis. World journal of gastroenterology. 2014;20(28):9458-67.
11. de Mattos B, Garcia M, Nogueira J, Paiatto L, Albuquerque C, Souza C, et al. Inflammatory Bowel Disease: An Overview of Immune Mechanisms and Biological Treatments. Mediators of inflammation. 2015;2015:493012.
12. Zundler S, Becker E, Schulze L, Neurath M. Immune cell trafficking and retention in inflammatory bowel disease: mechanistic insights and therapeutic advances. Gut. 2019;68(9):1688-700.
13. Morgan XC, Tickle TL, Sokol H, Gevers D, Devaney KL, Ward DV, et al. Dysfunction of the intestinal microbiome in inflammatory bowel disease and treatment. Genome biology. 2012;13(9):R79.
14. Schirmer M, Franzosa E, Lloyd-Price J, McIver L, Schwager R, Poon T, et al. Dynamics of metatranscription in the inflammatory bowel disease gut microbiome. Nature microbiology. 2018;3(3):337-46.

15. Parikh K, Antanaviciute A, Fawkner-Corbett D, Jagielowicz M, Aulicino A, Lagerholm C, et al. Colonic epithelial cell diversity in health and inflammatory bowel disease. Nature. 2019;567(7746):49-55.
16. Shen Z, Zhu C, Quan Y, Yang J, Yuan W, Yang Z, et al. Insights into Roseburia intestinalis which alleviates experimental colitis pathology by inducing anti-inflammatory responses. Journal of gastroenterology and hepatology. 2018;33(10):1751-60.
17. Belkaid Y, Hand TW. Role of the microbiota in immunity and inflammation. Cell. 2014;157(1):121-41.
18. Dai Y, Lu Q, Li P, Zhu J, Jiang J, Zhao T, et al. Xianglian Pill attenuates ulcerative colitis through TLR4/MyD88/NF-κB signaling pathway. Journal of ethnopharmacology. 2023;300:115690.
19. Neurath MF. Cytokines in inflammatory bowel disease. Nature reviews Immunology. 2014;14(5):329-42.
20. Biasi F, Leonarduzzi G, Oteiza PI, Poli G. Inflammatory bowel disease: mechanisms, redox considerations, and therapeutic targets. Antioxidants & redox signaling. 2013;19(14):1711-47.
21. Peng S, Shen L, Yu X, Zhang L, Xu K, Xia Y, et al. The role of Nrf2 in the pathogenesis and treatment of ulcerative colitis. Frontiers in immunology. 2023;14:1200111.
22. Xue JC, Yuan S, Hou XT, Meng H, Liu BH, Cheng WW, et al. Natural products modulate NLRP3 in ulcerative colitis. Frontiers in pharmacology. 2023;14:1265825.
23. Ding L, Yang L, Wang Z, Huang W. Bile acid nuclear receptor FXR and digestive system diseases. Acta pharmaceutica Sinica B. 2015;5(2):135-44.
24. Gibson GR, Hutkins R, Sanders ME, Prescott SL, Reimer RA, Salminen SJ, et al. Expert consensus document: The International Scientific Association for Probiotics and Prebiotics (ISAPP) consensus statement on the definition and scope of prebiotics. Nature reviews Gastroenterology & hepatology. 2017;14(8):491-502.
25. Kang Y, Kang X, Yang H, Liu H, Yang X, Liu Q, et al. Lactobacillus acidophilus ameliorates obesity in mice through modulation of gut microbiota dysbiosis and intestinal permeability. Pharmacological research. 2022;175:106020.
26. Liu C, Wang YL, Yang YY, Zhang NP, Niu C, Shen XZ, et al. Novel approaches to intervene gut microbiota in the treatment of chronic liver diseases. FASEB journal : official publication of the Federation of American Societies for Experimental Biology. 2021;35(10):e21871.
27. Jia DJ, Wang QW, Hu YY, He JM, Ge QW, Qi YD, et al. Lactobacillus johnsonii alleviates colitis by TLR1/2-STAT3 mediated CD206(+) macrophages(IL-10) activation. Gut microbes. 2022;14(1):2145843.
28. Kang Y, Ren P, Shen X, Kuang X, Yang X, Liu H, et al. A Newly Synbiotic Combination Alleviates Obesity by Modulating the Gut Microbiota-Fat Axis and Inhibiting the Hepatic TLR4/NF-κB Signaling Pathway. Molecular nutrition & food research. 2023;67(24):e2300141.
29. Song C, Wu J, Wu J, Wang F. MnO(2) and roflumilast-loaded probiotic membrane vesicles mitigate experimental colitis by synergistically augmenting cAMP in macrophage. Journal of nanobiotechnology. 2024;22(1):294.
30. Zhou S, Wang M, Li W, Zhang Y, Zhao T, Song Q, et al. Comparative efficacy and tolerability of probiotic, prebiotic, and synbiotic formulations for adult patients with mild-moderate ulcerative colitis in an adjunctive therapy: A network meta-analysis. Clinical nutrition (Edinburgh, Scotland). 2024;43(1):20-30.
31. Saggioro A. Probiotics in the treatment of irritable bowel syndrome. Journal of clinical gastroenterology. 2004;38(6 Suppl):S104-6.
32. Wang MX, Lin L, Chen YD, Zhong YP, Lin YX, Li P, et al. Evodiamine has therapeutic efficacy in ulcerative colitis by increasing Lactobacillus acidophilus levels and acetate production. Pharmacological research. 2020;159:104978.
33. Wu Y, Jha R, Li A, Liu H, Zhang Z, Zhang C, et al. Probiotics (Lactobacillus plantarum HNU082) Supplementation Relieves Ulcerative Colitis by Affecting Intestinal Barrier Functions, Immunity-Related Gene Expression, Gut Microbiota, and Metabolic Pathways in Mice. Microbiology spectrum. 2022;10(6):e0165122.
34. Fang X, Liu H, Du Y, Jiang L, Gao F, Wang Z, et al. Bacillus siamensis Targeted Screening from Highly Colitis-Resistant Pigs Can Alleviate Ulcerative Colitis in Mice. Research (Washington, DC). 2024;7:0415.
35. Kang Y, Kang X, Yang H, Liu H, Yang X, Liu Q, et al. Lactobacillus acidophilus ameliorates obesity in mice through modulation of gut microbiota dysbiosis and intestinal permeability. Pharmacological research. 2022;175:106020.
36. Liu Y, Sheng Y, Pan Q, Xue Y, Yu L, Tian F, et al. Identification of the key physiological characteristics of Lactobacillus plantarum strains for ulcerative colitis alleviation. Food & function. 2020;11(2):1279-91.

37. Li P, Chen G, Zhang J, Pei C, Chen Y, Gong J, et al. Lactobacillus acidophilusLive alleviates ulcerative colitis the SCFAs/mitophagy/NLRP3 inflammasome axis. Food & function. 2022;13(5):2985-97.
38. Kang Y, Ren P, Shen X, Kuang X, Yang X, Liu H, et al. A Newly Synbiotic Combination Alleviates Obesity by Modulating the Gut Microbiota-Fat Axis and Inhibiting the Hepatic TLR4/NF-κB Signaling Pathway. Molecular nutrition & food research. 2023;67(24):e2300141.
39. Qingqing L, Hao Y, Xing K, Haixia T, Yongbo K, Lin L, et al. A Synbiotic Ameliorates Con A-Induced Autoimmune Hepatitis in Mice through Modulation of Gut Microbiota and Immune Imbalance. Mol Nutr Food Res. 2023;67(7).
40. Song-Zi X, Bing L, Hui-Yu Y, Qiang-Ming L, Li-Hua P, Xue-Qiang Z, et al. Dendrobium huoshanense polysaccharide regionally regulates intestinal mucosal barrier function and intestinal microbiota in mice. Carbohydr Polym. 2018;206(0).
41. Jin X, Shimin T, Jun L, Shengjie H, Ming Y, Xiangbo Y, et al. Combination Therapy with Indigo and Indirubin for Ulcerative Colitis via Reinforcing Intestinal Barrier Function. Oxid Med Cell Longev. 2023;2023(0).
42. Liu F, Wang X, Li D, Cui Y, Li X. Apple polyphenols extract alleviated dextran sulfate sodium-induced ulcerative colitis in C57BL/6 male mice by restoring bile acid metabolism disorder and gut microbiota dysbiosis. Phytotherapy research : PTR. 2021;35(3):1468-85.
43. Alba R-N, Francesca A, Jose G-M, Teresa V, M Pilar U, Natalia C, et al. Differential intestinal anti-inflammatory effects of Lactobacillus fermentum and Lactobacillus salivarius in DSS mouse colitis: impact on microRNAs expression and microbiota composition. Mol Nutr Food Res. 2017;61(11).
44. Sun M, Liu Y, Song Y, Gao Y, Zhao F, Luo Y, et al. The ameliorative effect of Lactobacillus plantarum-12 on DSS-induced murine colitis. Food & function. 2020;11(6):5205-22.
45. Zhou Y, Ji G, Yang X, Chen Z, Zhou L. Behavioral abnormalities in C57BL/6 mice with chronic ulcerative colitis induced by DSS. BMC gastroenterology. 2023;23(1):84.
46. Gao J, Guo Z, Li W, Zhang X, Zhang XE, Cui Z. Ebola virus disrupts the inner blood-retinal barrier by induction of vascular endothelial growth factor in pericytes. PLoS pathogens. 2023;19(1):e1011077.
47. Koumangoye R, Omer S, Kabeer MH, Delpire E. Novel Human NKCC1 Mutations Cause Defects in Goblet Cell Mucus Secretion and Chronic Inflammation. Cellular and molecular gastroenterology and hepatology. 2020;9(2):239-55.
48. Tang M, Fang R, Xue J, Yang K, Lu Y. Effects of Catalase on Growth Performance, Antioxidant Capacity, Intestinal Morphology, and Microbial Composition in Yellow Broilers. Frontiers in veterinary science. 2022;9:802051.
49. Cheng H, Liu J, Zhang D, Wang J, Tan Y, Feng W, et al. Ginsenoside Rg1 Alleviates Acute Ulcerative Colitis by Modulating Gut Microbiota and Microbial Tryptophan Metabolism. Frontiers in immunology. 2022;13:817600.
50. Mar JS, LaMere BJ, Lin DL, Levan S, Nazareth M, Mahadevan U, et al. Disease Severity and Immune Activity Relate to Distinct Interkingdom Gut Microbiome States in Ethnically Distinct Ulcerative Colitis Patients. mBio. 2016;7(4).
51. Quagliariello A, Del Chierico F, Reddel S, Russo A, Onetti Muda A, D'Argenio P, et al. Fecal Microbiota Transplant in Two Ulcerative Colitis Pediatric Cases: Gut Microbiota and Clinical Course Correlations. Microorganisms. 2020;8(10).
52. He YF, Hu XM, Khan MA, Yu BY, Sheng YC, Xiao XZ, et al. HSF1 Alleviates Brain Injury by Inhibiting NLRP3-Induced Pyroptosis in a Sepsis Model. Mediators of inflammation. 2023;2023:2252255.
53. Dong Y, Fan H, Zhang Z, Jiang F, Li M, Zhou H, et al. Berberine ameliorates DSS-induced intestinal mucosal barrier dysfunction through microbiota-dependence and Wnt/β-catenin pathway. International journal of biological sciences. 2022;18(4):1381-97.
54. Pei LY, Ke YS, Zhao HH, Wang L, Jia C, Liu WZ, et al. Role of colonic microbiota in the pathogenesis of ulcerative colitis. BMC gastroenterology. 2019;19(1):10.
55. Geng ZH, Zhu Y, Li QL, Zhao C, Zhou PH. Enteric Nervous System: The Bridge Between the Gut Microbiota and Neurological Disorders. Frontiers in aging neuroscience. 2022;14:810483.
56. Ye M, Hou M, Peng Q, Jia S, Peng B, Yin F, et al. The Microbiota and Cytokines Correlation between the Jejunum and Colon in Altay Sheep. Animals : an open access journal from MDPI. 2022;12(12).
57. Geng B, Ding X, Li X, Liu H, Zhao W, Gong H, et al. Peripheral blood T-lymphocyte subsets are potential biomarkers of disease severity and clinical outcomes in patients with ulcerative colitis: a retrospective study. BMC gastroenterology. 2023;23(1):136.

58. Ray MK, Fenton CG, Paulssen RH. Novel long non-coding RNAs of relevance for ulcerative colitis pathogenesis. Non-coding RNA research. 2022;7(1):40-7.
59. Tu Z, Xue H, Chen W, Cao L, Zhang W. Changes of Treg and Th17 cells as well as cytokines in children with acute bronchitis. Experimental and therapeutic medicine. 2017;14(4):3846-50.
60. Van Nguyen T, Piao CH, Fan YJ, Shin DU, Kim SY, Song HJ, et al. Anti-allergic rhinitis activity of α-lipoic acid via balancing Th17/Treg expression and enhancing Nrf2/HO-1 pathway signaling. Scientific reports. 2020;10(1):12528.
61. Xie J, Tian S, Liu J, Huang S, Yang M, Yang X, et al. Combination Therapy with Indigo and Indirubin for Ulcerative Colitis via Reinforcing Intestinal Barrier Function. Oxidative medicine and cellular longevity. 2023;2023:2894695.
62. Allaire JM, Crowley SM, Law HT, Chang SY, Ko HJ, Vallance BA. The Intestinal Epithelium: Central Coordinator of Mucosal Immunity. Trends in immunology. 2018;39(9):677-96.
63. Basso L, Boué J, Augé C, Deraison C, Blanpied C, Cenac N, et al. Mobilization of CD4+ T lymphocytes in inflamed mucosa reduces pain in colitis mice: toward a vaccinal strategy to alleviate inflammatory visceral pain. Pain. 2018;159(2):331-41.
64. Corridoni D, Antanaviciute A, Gupta T, Fawkner-Corbett D, Aulicino A, Jagielowicz M, et al. Single-cell atlas of colonic CD8(+) T cells in ulcerative colitis. Nature medicine. 2020;26(9):1480-90.
65. Hirata I, Berrebi G, Austin LL, Keren DF, Dobbins WO, 3rd. Immunohistological characterization of intraepithelial and lamina propria lymphocytes in control ileum and colon and in inflammatory bowel disease. Digestive diseases and sciences. 1986;31(6):593-603.
66. Schreiber S, MacDermott RP, Raedler A, Pinnau R, Bertovich MJ, Nash GS. Increased activation of isolated intestinal lamina propria mononuclear cells in inflammatory bowel disease. Gastroenterology. 1991;101(4):1020-30.
67. Zhu J, Xu Y, Li Z, Liu S, Fu W, Wei Y. Interleukin-36β exacerbates DSS-induce acute colitis via inhibiting Foxp3(+) regulatory T cell response and increasing Th2 cell response. International immunopharmacology. 2022;108:108762.
68. Zhu JF, Xu Y, Zhao J, Li X, Meng X, Wang TQ, et al. IL-33 Protects Mice against DSS-Induced Chronic Colitis by Increasing Both Regulatory B Cell and Regulatory T Cell Responses as Well as Decreasing Th17 Cell Response. Journal of immunology research. 2018;2018:1827901.
69. Yang CC, Hsiao LD, Lin HH, Tseng HC, Situmorang JH, Leu YL, et al. Induction of HO-1 by 5, 8-Dihydroxy-4',7-Dimethoxyflavone via Activation of ROS/p38 MAPK/Nrf2 Attenuates Thrombin-Induced Connective Tissue Growth Factor Expression in Human Cardiac Fibroblasts. Oxidative medicine and cellular longevity. 2020;2020:1080168.
70. Zhang L, Gui S, Xu Y, Zeng J, Wang J, Chen Q, et al. Colon tissue-accumulating mesoporous carbon nanoparticles loaded with Musca domestica cecropin for ulcerative colitis therapy. Theranostics. 2021;11(7):3417-38.
71. Chen YF, Zheng JJ, Qu C, Xiao Y, Li FF, Jin QX, et al. Inonotus obliquus polysaccharide ameliorates dextran sulphate sodium induced colitis involving modulation of Th1/Th2 and Th17/Treg balance. Artificial cells, nanomedicine, and biotechnology. 2019;47(1):757-66.
72. Zhou X, Cao L, Jiang C, Xie Y, Cheng X, Krausz K, et al. PPARα-UGT axis activation represses intestinal FXR-FGF15 feedback signalling and exacerbates experimental colitis. Nature communications. 2014;5:4573.
73. Shen F, Feng J, Wang X, Qi Z, Shi X, An Y, et al. Vinegar Treatment Prevents the Development of Murine Experimental Colitis via Inhibition of Inflammation and Apoptosis. Journal of agricultural and food chemistry. 2016;64(5):1111-21.
74. Zhang Z, Shen P, Lu X, Li Y, Liu J, Liu B, et al. In Vivo and In Vitro Study on the Efficacy of Terpinen-4-ol in Dextran Sulfate Sodium-Induced Mice Experimental Colitis. Frontiers in immunology. 2017;8:558.
75. Dai N, Yang X, Pan P, Zhang G, Sheng K, Wang J, et al. Bacillus paralicheniformis, an acetate-producing probiotic, alleviates ulcerative colitis via protecting the intestinal barrier and regulating the NLRP3 inflammasome. Microbiological Research. 2024;287:127856.
76. Hrdý J, Couturier-Maillard A, Boutillier D, Lapadatescu C, Blanc P, Procházka J, et al. Oral supplementation with selected Lactobacillus acidophilus triggers IL-17-dependent innate defense response, activation of innate lymphoid cells type 3 and improves colitis. Scientific Reports. 2022;12(1):17591.

77. Kang Y, Kuang X, Yan H, Ren P, Yang X, Liu H, et al. A Novel Synbiotic Alleviates Autoimmune Hepatitis by Modulating the Gut Microbiota-Liver Axis and Inhibiting the Hepatic TLR4/NF-κB/NLRP3 Signaling Pathway. mSystems. 2023;8(2):e0112722.
78. Kang Y, Li Y, Du Y, Guo L, Chen M, Huang X, et al. Konjaku flour reduces obesity in mice by modulating the composition of the gut microbiota. International journal of obesity (2005). 2019;43(8):1631-43.
79. Ordás I, Eckmann L, Talamini M, Baumgart DC, Sandborn WJ. Ulcerative colitis. Lancet (London, England). 2012;380(9853):1606-19.
80. Krugliak Cleveland N, Torres J, Rubin DT. What Does Disease Progression Look Like in Ulcerative Colitis, and How Might It Be Prevented? Gastroenterology. 2022;162(5):1396-408.
81. Pawłowska B, Sobieszczańska BM. Intestinal epithelial barrier: The target for pathogenic Escherichia coli. Advances in clinical and experimental medicine : official organ Wroclaw Medical University. 2017;26(9):1437-45.
82. Garcia-Hernandez V, Quiros M, Nusrat A. Intestinal epithelial claudins: expression and regulation in homeostasis and inflammation. Annals of the New York Academy of Sciences. 2017;1397(1):66-79.
83. Wu Y, Jha R, Li A, Liu H, Zhang Z, Zhang C, et al. Probiotics (Lactobacillus plantarum HNU082) Supplementation Relieves Ulcerative Colitis by Affecting Intestinal Barrier Functions, Immunity-Related Gene Expression, Gut Microbiota, and Metabolic Pathways in Mice. Microbiology spectrum. 2022;10(6):e0165122.
84. Xie SZ, Liu B, Ye HY, Li QM, Pan LH, Zha XQ, et al. Dendrobium huoshanense polysaccharide regionally regulates intestinal mucosal barrier function and intestinal microbiota in mice. Carbohydrate polymers. 2019;206:149-62.
85. Hansen J, Gulati A, Sartor RB. The role of mucosal immunity and host genetics in defining intestinal commensal bacteria. Current opinion in gastroenterology. 2010;26(6):564-71.
86. Ohkusa T, Koido S. Intestinal microbiota and ulcerative colitis. Journal of infection and chemotherapy : official journal of the Japan Society of Chemotherapy. 2015;21(11):761-8.
87. Gao H, Li Y, Sun J, Xu H, Wang M, Zuo X, et al. Saccharomyces boulardii Ameliorates Dextran Sulfate Sodium-Induced Ulcerative Colitis in Mice by Regulating NF-κB and Nrf2 Signaling Pathways. Oxidative medicine and cellular longevity. 2021;2021:1622375.
88. Li N, Wang H, Zhao H, Wang M, Cai J, Hao Y, et al. Cooperative interactions between Veillonella ratti and Lactobacillus acidophilus ameliorate DSS-induced ulcerative colitis in mice. Food Funct. 2023;14(23):10475-92.
89. Sun S, Xu X, Liang L, Wang X, Bai X, Zhu L, et al. Lactic Acid-Producing Probiotic Saccharomyces cerevisiae Attenuates Ulcerative Colitis via Suppressing Macrophage Pyroptosis and Modulating Gut Microbiota. Frontiers in immunology. 2021;12:777665.
90. Ikeda E, Yamaguchi M, Kawabata S. Gut Microbiota-mediated Alleviation of Dextran Sulfate Sodium-induced Colitis in Mice. Gastro hep advances. 2024;3(4):461-70.
91. Fabian R-C, Lillian F Z, Franziska F, Christopher A L, Mariana X B, Erin E O, et al. Depletion of Butyrate-Producing Clostridia from the Gut Microbiota Drives an Aerobic Luminal Expansion of Salmonella. Cell Host Microbe.19(4).
92. Julia D, Floyd E D, Anne C R T, William G W. Description of Alloprevotella rava gen. nov., sp. nov., isolated from the human oral cavity, and reclassification of Prevotella tannerae Moore et al. 1994 as Alloprevotella tannerae gen. nov., comb. nov. Int J Syst Evol Microbiol. 2012;63(0).
93. Cheng WY, Lam KL, Li X, Kong AP, Cheung PC. Circadian disruption-induced metabolic syndrome in mice is ameliorated by oat β-glucan mediated by gut microbiota. Carbohydrate polymers. 2021;267:118216.
94. Niu X, Shang H, Chen S, Chen R, Huang J, Miao Y, et al. Effects of Pinus massoniana pollen polysaccharides on intestinal microenvironment and colitis in mice. Food & function. 2021;12(1):252-66.
95. Mirco V, Giuseppe C, Francesco Maria C, Piero P, Marco G, Maria DA. The Controversial Role of Human Gut Lachnospiraceae. Microorganisms. 2020;8(4).
96. Zhang L, Li X, Liu X, Wu X, Xu Q, Qu J, et al. High-Carbohydrate Diet Consumption Poses a More Severe Liver Cholesterol Deposition than a High-Fat and High-Calorie Diet in Mice. International journal of molecular sciences. 2023;24(19).
97. Wang X, Fan F, Cao Q. Modified Pulsatilla decoction attenuates oxazolone-induced colitis in mice through suppression of inflammation and epithelial barrier disruption. Molecular medicine reports. 2016;14(2):1173-9.

98. Hong J, Fu T, Liu W, Du Y, Bu J, Wei G, et al. Jiangtang Decoction Ameliorates Diabetic Kidney Disease Through the Modulation of the Gut Microbiota. Diabetes, metabolic syndrome and obesity : targets and therapy. 2023;16:3707-25.
99. Pang B, Jin H, Liao N, Li J, Jiang C, Shi J. Vitamin A supplementation ameliorates ulcerative colitis in gut microbiota-dependent manner. Food research international (Ottawa, Ont). 2021;148:110568.
100. Peng L, Gao X, Nie L, Xie J, Dai T, Shi C, et al. Astragalin Attenuates Dextran Sulfate Sodium (DSS)-Induced Acute Experimental Colitis by Alleviating Gut Microbiota Dysbiosis and Inhibiting NF-κB Activation in Mice. Frontiers in immunology. 2020;11:2058.
101. Shang L, Liu H, Yu H, Chen M, Yang T, Zeng X, et al. Core Altered Microorganisms in Colitis Mouse Model: A Comprehensive Time-Point and Fecal Microbiota Transplantation Analysis. Antibiotics (Basel, Switzerland). 2021;10(6).
102. Shao J, Li Z, Gao Y, Zhao K, Lin M, Li Y, et al. Construction of a "Bacteria-Metabolites" Co-Expression Network to Clarify the Anti-Ulcerative Colitis Effect of Flavonoids of Sophora flavescens Aiton by Regulating the "Host-Microbe" Interaction. Frontiers in pharmacology. 2021;12:710052.
103. Niu W, Dong Y, Fu Z, Lv J, Wang L, Zhang Z, et al. Effects of molecular weight of chitosan on anti-inflammatory activity and modulation of intestinal microflora in an ulcerative colitis model. International journal of biological macromolecules. 2021;193(Pt B):1927-36.
104. Chang S, Song M, Lee J, Oh H, Kim Y, An J, et al. Phytogenic feed additives alleviate pathogenic Escherichia coli-induced intestinal damage through improving barrier integrity and inhibiting inflammation in weaned pigs. Journal of animal science and biotechnology. 2022;13(1):107.
105. Kim HY, Bae CH, Kim J, Lee Y, Jeon H, Kim H, et al. Rumex japonicus Houtt. Protects Dopaminergic Neurons by Regulating Mitochondrial Function and Gut-Brain Axis in In Vitro and In Vivo Models of Parkinson's Disease. Antioxidants (Basel, Switzerland). 2022;11(1).
106. Ou YH, Liang J, Chng WH, Muthuramalingam RPK, Ng ZX, Lee CK, et al. Investigations on Cellular Uptake Mechanisms and Immunogenicity Profile of Novel Bio-Hybrid Nanovesicles. Pharmaceutics. 2022;14(8).
107. Caza T, Landas S. Functional and Phenotypic Plasticity of CD4(+) T Cell Subsets. BioMed research international. 2015;2015:521957.
108. Raphael I, Nalawade S, Eagar TN, Forsthuber TG. T cell subsets and their signature cytokines in autoimmune and inflammatory diseases. Cytokine. 2015;74(1):5-17.
109. Alfen JS, Larghi P, Facciotti F, Gagliani N, Bosotti R, Paroni M, et al. Intestinal IFN-γ-producing type 1 regulatory T cells coexpress CCR5 and programmed cell death protein 1 and downregulate IL-10 in the inflamed guts of patients with inflammatory bowel disease. The Journal of allergy and clinical immunology. 2018;142(5):1537-47.e8.
110. Li X, Wang Q, Ding L, Wang YX, Zhao ZD, Mao N, et al. Intercellular adhesion molecule-1 enhances the therapeutic effects of MSCs in a dextran sulfate sodium-induced colitis models by promoting MSCs homing to murine colons and spleens. Stem cell research & therapy. 2019;10(1):267.
111. Chen L, He Z, Reis BS, Gelles JD, Chipuk JE, Ting AT, et al. IFN-γ(+) cytotoxic CD4(+) T lymphocytes are involved in the pathogenesis of colitis induced by IL-23 and the food colorant Red 40. Cellular & molecular immunology. 2022;19(7):777-90.
112. Alipour M, Lou Y, Zimmerman D, Bording-Jorgensen M, Sergi C, Liu J, et al. A balanced IL-1β activity is required for host response to Citrobacter rodentium infection. PloS one. 2013;8(12):e80656.
113. Hasegawa M, Kamada N, Jiao Y, Liu M, Núñez G, Inohara N. Protective role of commensals against Clostridium difficile infection via an IL-1β-mediated positive-feedback loop. Journal of immunology (Baltimore, Md : 1950). 2012;189(6):3085-91.
114. He Y, Hara H, Núñez G. Mechanism and Regulation of NLRP3 Inflammasome Activation. Trends in biochemical sciences. 2016;41(12):1012-21.
115. Rawat M, Nighot M, Al-Sadi R, Gupta Y, Viszwapriya D, Yochum G, et al. IL1B Increases Intestinal Tight Junction Permeability by Up-regulation of MIR200C-3p, Which Degrades Occludin mRNA. Gastroenterology. 2020;159(4):1375-89.
116. Guo HW, Yun CX, Hou GH, Du J, Huang X, Lu Y, et al. Mangiferin attenuates TH1/TH2 cytokine imbalance in an ovalbumin-induced asthmatic mouse model. PloS one. 2014;9(6):e100394.
117. Zhang L, Zhang Y, Zhong W, Di C, Lin X, Xia Z. Heme oxygenase-1 ameliorates dextran sulfate sodium-induced acute murine colitis by regulating Th17/Treg cell balance. The Journal of biological chemistry. 2014;289(39):26847-58.

118. Aparicio-Domingo P, Romera-Hernandez M, Karrich JJ, Cornelissen F, Papazian N, Lindenbergh-Kortleve DJ, et al. Type 3 innate lymphoid cells maintain intestinal epithelial stem cells after tissue damage. The Journal of experimental medicine. 2015;212(11):1783-91.
119. Lindemans CA, Calafiore M, Mertelsmann AM, O'Connor MH, Dudakov JA, Jenq RR, et al. Interleukin-22 promotes intestinal-stem-cell-mediated epithelial regeneration. Nature. 2015;528(7583):560-4.
120. Josefowicz SZ, Lu LF, Rudensky AY. Regulatory T cells: mechanisms of differentiation and function. Annual review of immunology. 2012;30:531-64.
121. Ueno A, Jijon H, Chan R, Ford K, Hirota C, Kaplan GG, et al. Increased prevalence of circulating novel IL-17 secreting Foxp3 expressing CD4+ T cells and defective suppressive function of circulating Foxp3+ regulatory cells support plasticity between Th17 and regulatory T cells in inflammatory bowel disease patients. Inflammatory bowel diseases. 2013;19(12):2522-34.
122. Shi X, Huang H, Zhou M, Liu Y, Wu H, Dai M. Paeonol Attenuated Vascular Fibrosis Through Regulating Treg/Th17 Balance in a Gut Microbiota-Dependent Manner. Frontiers in pharmacology. 2021;12:765482.
123. Wang S, Ruan P, Peng L, Wang J. Cytokine-stimulated human amniotic epithelial cells alleviate DSS-induced colitis in mice through anti-inflammation and regulating Th17/Treg balance. International immunopharmacology. 2023;120:110265.
124. Dong S, Zhu M, Wang K, Zhao X, Hu L, Jing W, et al. Dihydromyricetin improves DSS-induced colitis in mice via modulation of fecal-bacteria-related bile acid metabolism. Pharmacological research. 2021;171:105767.
125. Alkushi AG, Elazab ST, Abdelfattah-Hassan A, Mahfouz H, Salem GA, Sheraiba NI, et al. Multi-Strain-Probiotic-Loaded Nanoparticles Reduced Colon Inflammation and Orchestrated the Expressions of Tight Junction, NLRP3 Inflammasome and Caspase-1 Genes in DSS-Induced Colitis Model. Pharmaceutics. 2022;14(6).
126. Trevisin M, Pollock W, Dimech W, Savige J. Evaluation of a multiplex flow cytometric immunoassay to detect PR3- and MPO-ANCA in active and treated vasculitis, and in inflammatory bowel disease (IBD). Journal of immunological methods. 2008;336(2):104-12.
127. Arnhold J. The Dual Role of Myeloperoxidase in Immune Response. International journal of molecular sciences. 2020;21(21).
128. Wardyn JD, Ponsford AH, Sanderson CM. Dissecting molecular cross-talk between Nrf2 and NF-κB response pathways. Biochemical Society transactions. 2015;43(4):621-6.
129. Ramakrishnan SK, Zhang H, Ma X, Jung I, Schwartz AJ, Triner D, et al. Intestinal non-canonical NFκB signaling shapes the local and systemic immune response. Nature communications. 2019;10(1):660.
130. Saber S, Khalil RM, Abdo WS, Nassif D, El-Ahwany E. Olmesartan ameliorates chemically-induced ulcerative colitis in rats via modulating NFκB and Nrf-2/HO-1 signaling crosstalk. Toxicology and applied pharmacology. 2019;364:120-32.
131. Fu YJ, Xu B, Huang SW, Luo X, Deng XL, Luo S, et al. Baicalin prevents LPS-induced activation of TLR4/NF-κB p65 pathway and inflammation in mice via inhibiting the expression of CD14. Acta pharmacologica Sinica. 2021;42(1):88-96.
132. Dayalan Naidu S, Dinkova-Kostova AT. KEAP1, a cysteine-based sensor and a drug target for the prevention and treatment of chronic disease. Open biology. 2020;10(6):200105.
133. Geertsema S, Bourgonje AR, Fagundes RR, Gacesa R, Weersma RK, van Goor H, et al. The NRF2/Keap1 pathway as a therapeutic target in inflammatory bowel disease. Trends in molecular medicine. 2023;29(10):830-42.
134. Liu GH, Qu J, Shen X. NF-kappaB/p65 antagonizes Nrf2-ARE pathway by depriving CBP from Nrf2 and facilitating recruitment of HDAC3 to MafK. Biochimica et biophysica acta. 2008;1783(5):713-27.
135. Liu D, Huo X, Gao L, Zhang J, Ni H, Cao L. NF-κB and Nrf2 pathways contribute to the protective effect of Licochalcone A on dextran sulphate sodium-induced ulcerative colitis in mice. Biomedicine & pharmacotherapy = Biomedecine & pharmacotherapie. 2018;102:922-9.
136. Thimmulappa RK, Lee H, Rangasamy T, Reddy SP, Yamamoto M, Kensler TW, et al. Nrf2 is a critical regulator of the innate immune response and survival during experimental sepsis. The Journal of clinical investigation. 2006;116(4):984-95.
137. Frakes AE, Ferraiuolo L, Haidet-Phillips AM, Schmelzer L, Braun L, Miranda CJ, et al. Microglia induce motor neuron death via the classical NF-κB pathway in amyotrophic lateral sclerosis. Neuron. 2014;81(5):1009-23.
138. Hu J, Huang H, Che Y, Ding C, Zhang L, Wang Y, et al. Qingchang Huashi Formula attenuates DSS-induced colitis in mice by restoring gut microbiota-metabolism homeostasis and goblet cell function. Journal of ethnopharmacology. 2021;266:113394.

139. Copple BL, Li T. Pharmacology of bile acid receptors: Evolution of bile acids from simple detergents to complex signaling molecules. Pharmacological research. 2016;104:9-21.
140. Kir S, Zhang Y, Gerard RD, Kliewer SA, Mangelsdorf DJ. Nuclear receptors HNF4α and LRH-1 cooperate in regulating Cyp7a1 in vivo. The Journal of biological chemistry. 2012;287(49):41334-41.
141. Duan Y, Zhang F, Yuan W, Wei Y, Wei M, Zhou Y, et al. Hepatic cholesterol accumulation ascribed to the activation of ileum Fxr-Fgf15 pathway inhibiting hepatic Cyp7a1 in high-fat diet-induced obesity rats. Life sciences. 2019;232:116638.
142. Tayyar AT, Tayyar A, Kozali S, Karakus R, Koroglu N, Yuksel IT, et al. Evaluation of FGF-19 and β-klotho as biomarkers in patients with intrahepatic cholestasis of pregnancy. Archives of medical science : AMS. 2019;15(1):113-9.
143. Tang K, Kong D, Peng Y, Guo J, Zhong Y, Yu H, et al. Ginsenoside Rc attenuates DSS-induced ulcerative colitis, intestinal inflammatory, and barrier function by activating the farnesoid X receptor. Frontiers in pharmacology. 2022;13:1000444.
144. Xiao Y, Jia YQ, Liu WJ, Niu C, Mai ZH, Dong JQ, et al. Pulsatilla decoction alleviates DSS-induced UC by activating FXR-ASBT pathways to ameliorate disordered bile acids homeostasis. Front Pharmacol. 2024;15:1399829.
145. Shen HH, Yang YX, Meng X, Luo XY, Li XM, Shuai ZW, et al. NLRP3: A promising therapeutic target for autoimmune diseases. Autoimmunity reviews. 2018;17(7):694-702.
146. Jo EK, Kim JK, Shin DM, Sasakawa C. Molecular mechanisms regulating NLRP3 inflammasome activation. Cellular & molecular immunology. 2016;13(2):148-59.
147. Huang Y, Xu W, Zhou R. NLRP3 inflammasome activation and cell death. Cellular & Molecular Immunology. 2021;18(9):2114-27.
148. Shi J, Zhao Y, Wang K, Shi X, Wang Y, Huang H, et al. Cleavage of GSDMD by inflammatory caspases determines pyroptotic cell death. Nature. 2015;526(7575):660-5.
149. Bauer C, Duewell P, Mayer C, Lehr HA, Fitzgerald KA, Dauer M, et al. Colitis induced in mice with dextran sulfate sodium (DSS) is mediated by the NLRP3 inflammasome. Gut. 2010;59(9):1192-9.
150. Chen X, Liu G, Yuan Y, Wu G, Wang S, Yuan L. NEK7 interacts with NLRP3 to modulate the pyroptosis in inflammatory bowel disease via NF-κB signaling. Cell death & disease. 2019;10(12):906.
151. Lv Q, Xing Y, Liu J, Dong D, Liu Y, Qiao H, et al. Lonicerin targets EZH2 to alleviate ulcerative colitis by autophagy-mediated NLRP3 inflammasome inactivation. Acta pharmaceutica Sinica B. 2021;11(9):2880-99.